Chapter 9

Tracking Radar

Dean D. Howard

Consultant to ITT Industries, Inc.

9.1 INTRODUCTION

Typical tracking radars have a pencil beam to receive echoes from a single target and track the target in angle, range, and/or doppler. Its resolution cell—defined by its antenna beamwidth, transmitter pulse length (effective pulse length may be shorter with pulse compression), and/or doppler bandwidth—is usually small compared with that of a search radar and is used to exclude undesired echoes or signals from other targets, clutter, and countermeasures. Electronic beam-scanning phased array radars may track multiple targets by sequentially dwelling upon and measuring each target while excluding other echo or signal sources.

Because of its narrow beamwidth, typically from a fraction of 1° to 1 or 2°, tracking radars usually depend upon information from a surveillance radar or other source of target location to acquire the target, i.e., to place its beam on or in the vicinity of the target before initiating a track. Scanning of the beam within a limited angle sector may be needed to acquire the target within its beam and center the range-tracking gates on the echo pulse prior to locking on the target or closing the tracking loops. The gate acts like a fast-acting on-off switch that turns the receiver "on" at the leading edge of the target echo pulse and "off" at the end of the target echo pulse to eliminate undesired echoes. The range-tracking system performs the task of keeping the gate centered on the target echo, as described in Section 9.5.

The primary output of tracking radar is the target location determined from the pointing angles of the beam and position of its range-tracking gates. The angle location is the data obtained from synchros and encoders on the antenna tracking axes (or data from a beam-positioning computer on an electronic-scan phased array radar). In some cases, tracking lag is measured by converting tracking-lag-error voltages from the tracking loops to units of angle. This data is used to add to or subtract from the angle shaft position data for real-time correction of tracking lag.

There are a large variety of tracking-radar systems, including some that achieve simultaneously both surveillance and tracking functions. A widely used type of tracking radar and the one discussed in detail in this chapter is a ground-based system consisting of a pencil-beam antenna mounted on a rotatable platform with servo motor drive of its azimuth and elevation position to follow a target (Figure 9.1*a*). Errors in pointing direction are determined by sensing the angle of arrival of the echo wavefront and corrected by positioning the antenna to keep the target centered

in the beam. Modern requirements for simultaneous precision tracking of multiple targets has driven the development of the electronic scan array monopulse radar with the capability to switch its beam pulse-to-pulse among multiple targets. The AN/MPS-39 shown in Figure 9.1*b* is an example of a highly versatile electronic scan monopulse missile-range instrumentation radar.

The principal applications of precision tracking radar are weapon control and missile-range instrumentation. In both applications, a high degree of precision and an accurate prediction of future position of the target are generally required. The earliest use of tracking radar was gunfire control. The azimuth angle, elevation angle, and the range to the target were measured, and from the rate of change of these parameters, the velocity vector of the target (speed and direction) was computed and its future position predicted. This information was used to move the gun to lead the target and set the fuze delay. The tracking radar performs a similar role in providing guidance information and steering commands for missile control.

In missile-range instrumentation, the tracking-radar output is used to measure the trajectory of the missile and to predict future position. Tracking radars are used to compute the impact point of a launched missile continuously during the launch phase in case of missile failure for range safety. If the impact point approaches a populated or other critical area, the missile is destroyed. Missile-range instrumentation radars are normally used with a beacon (pulse repeater) to provide a point-source echo—usually its pulse is delayed to separate it from the target echo—and with high signal-to-noise ratio, to achieve precision tracking on the order of 0.05 mil in angle and 5 m in range.

(a)

(b)

FIGURE 9.1 (*a*) AN/FPQ-6 C-band monopulse precision tracking radar installation at the NASA Wallops Island Station, VA. It has a 29-ft-diameter dish and a specified tracking precision of 0.05 mrad rms. (*b*) AN/MPS-39 C-band electronic scan phased-array Multi Object Tracking Radar (MOTR) installed at the White Sands Missile Range. (*Photo of the AN/MPS-39 courtesy of the White Sands Missile Range and Lockheed Martin.*)

This chapter describes the monopulse (simultaneous lobing with either phase comparison or amplitude comparison), conical-scan, and sequential lobing tracking-radar techniques with the main emphasis on the amplitude-comparison monopulse (simultaneous lobing) radar.

9.2 MONOPULSE (SIMULTANEOUS LOBING)

The susceptibility of conical scanning and sequential lobing tracking techniques to echo amplitude fluctuations and amplitude jamming (as described in Section 9.3) was the major reason for the development of tracking radar that provides simultaneously all the necessary lobes for angle-error sensing. This required that the output from the lobes be compared simultaneously on a single pulse, eliminating the effects of echo amplitude change with time. The technique to accomplish this was initially called *simultaneous lobing,* which was descriptive of the technique. Later, the term *monopulse* was coined, referring to the ability to obtain angle error information on a single pulse. It has become the commonly used name for this tracking technique; even though, the lobes are generated simultaneously and *monopulse* tracking can be performed with CW radar.

The original monopulse tracking radars suffered in antenna efficiency and complexity of microwave circuitry because waveguide signal-combining circuitry was a relatively new art. These problems were overcome and monopulse radar, with modern compact off-the-shelf processing circuitry, can readily outperform scanning and lobing systems. The monopulse technique also has an inherent capability for high-precision angle measurement because its feed structure is compact with short signal paths and rigidly mounted with no moving parts. This has made possible the development of pencil-beam tracking radars that meet missile-range instrumentation-radar requirements of 0.003° angle-tracking precision.

This chapter is devoted to tracking radar, but monopulse techniques are used in other systems including homing devices, direction finders, and some search radars. However, most of the basic principles and limitations of monopulse apply for all applications. More general coverage is found in Sherman[1] and Leonov and Formichev.[2]

Amplitude-Comparison Monopulse. A method for visualizing the operation of an amplitude-comparison receiver is to consider the echo signal at the focal plane of an antenna.[3] The echo is focused to a finite size "spot." The "spot" is centered on the focal plane when the target is on the antenna axis and moves off center when the target moves off axis. The antenna feed is located at the focal point to receive maximum energy from a target on axis.

The amplitude-comparison feed is designed to sense any feed plane displacement of the spot from the center of the focal plane. A monopulse feed using the four-horn square, for example, would be centered at the focal plane. It provides symmetry so that when the spot is centered, equal energy falls on each of the four horns. The radar senses target displacement from the antenna axis that shifts the spot off of the center of the focal plane by measuring the resultant unbalance of energy received in the four horns. This is accomplished by use of microwave waveguide hybrids to subtract outputs of pairs of horns, providing a sensitive device that gives signal output when there is an unbalance caused by the target being off axis. The RF circuitry for a conventional four-horn square feed (see Figure 9.2) subtracts the output of

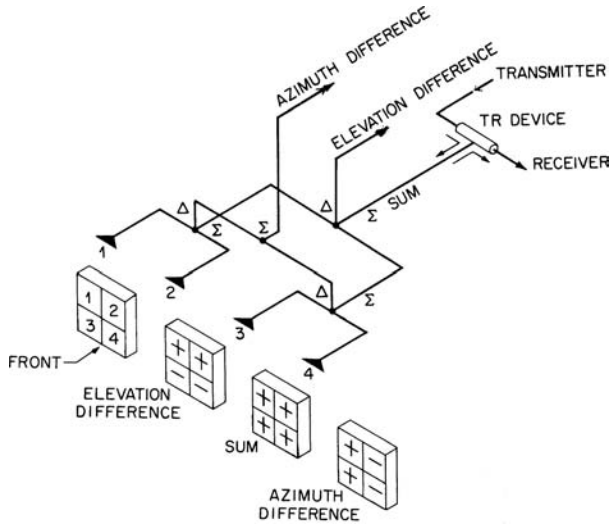

FIGURE 9.2 Microwave-comparator circuitry used with a four-horn monopulse feed

the left pair from the output of the right pair to sense any unbalance in the azimuth direction. It also subtracts the output of the top pair from the output of the bottom pair to sense any unbalance in the elevation direction. In addition, the circuitry adds the output of all four horns for a sum signal for detection, monopulse processing, and range tracking.

The comparator shown in Figure 9.2 is the circuitry that performs the addition and subtraction of the feed horn outputs to obtain monopulse sum and difference signals. It is illustrated with hybrid-T (or magic-T) waveguide components. These are four-port devices that, in basic form, have the inputs and outputs located at right angles to each other. However, the magic T's have been developed in convenient "folded" configurations for a very compact comparator. The performance of these and other similar four-port devices is described in Chapter 4 of Sherman.[1]

The subtractor outputs are called *difference signals,* which are zero when the target is on axis, increasing in amplitude with increasing displacement of the target from the antenna axis. The difference signals also change 180° in phase from one side of center to the other. The sum of all four-horn outputs provides a reference signal to control angle-tracking sensitivity (volts per degree of error) to remain constant, even though the target echo signal may vary over a large dynamic range. This is accomplished by automatic gain control (AGC) to keep the sum signal output and angle-tracking loop gains constant for stable automatic angle tracking.

Figure 9.3 is a block diagram of typical monopulse radars. The sum signal, elevation difference signal, and azimuth difference signal are each converted to intermediate frequency (IF), using a common local oscillator to maintain relative phase at IF. The IF sum-signal output is detected and provides the video input to the range tracker. The range tracker measures and tracks the time of arrival of the desired target echo and provides gate pulses that turn on the radar receiver channels only during the brief period when the desired echo is expected. The gated video is used to generate the dc

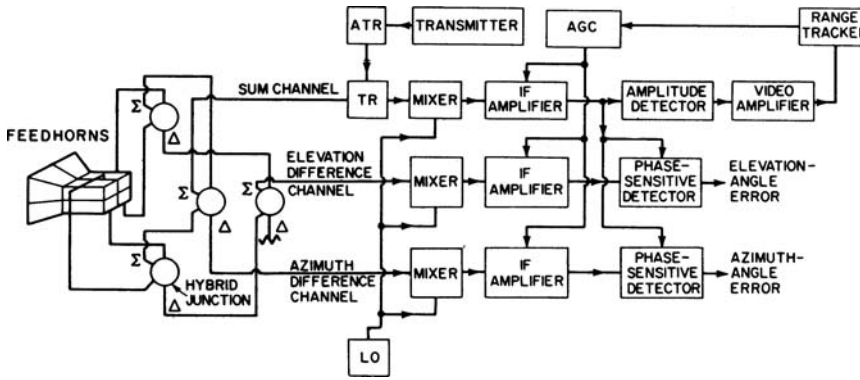

FIGURE 9.3 Block diagram of a conventional monopulse tracking radar

voltage proportional to the magnitude of the Σ signal or $|\Sigma|$ for the AGC of all three IF amplifier channels. The AGC maintains constant angle-tracking sensitivity (volts per degree error), even though the target echo signal varies over a large dynamic range, by controlling gain or dividing by $|\Sigma|$. AGC is necessary to keep the gain of the angle-tracking loops constant for stable automatic angle tracking. Some monopulse systems, such as the two-channel monopulse, can provide instantaneous AGC or normalizing by use of log detectors as described later in this section.

The sum signal at the IF output also provides a reference signal to phase detectors that derive angle-tracking-error voltages from the difference signals. The phase detectors are essentially dot-product devices producing the output voltage

$$e = \frac{|\Sigma|\,|\Delta|}{|\Sigma|\,|\Delta|}\cos\theta \qquad \text{or} \qquad e = \frac{\Delta}{|\Sigma|}\cos\theta \tag{9.1}$$

where e = angle-error-detector output voltage
$|\Sigma|$ = magnitude of sum signal
$|\Delta|$ = magnitude of difference signal
θ = phase angle between sum and difference signals

The dot-product error detector is only one of a wide variety of monopulse angle-error detectors described in Chapter 7 of Sherman.[1]

Normally, θ is either 0° or 180° when the radar is properly adjusted, and the only purpose of the phase-sensitive characteristic is to provide a plus or minus polarity corresponding to $\theta = 0°$ and $\theta = 180°$, respectively, giving a + or – polarity to the angle-error-detector output to indicate to the servo which direction to drive the pedestal.

In a pulsed tracking radar, the angle-error-detector output is bipolar video; that is, it is a video pulse with an amplitude proportional to the angle error and whose polarity (positive or negative) corresponds to the direction of the error. This video is typically processed by a sample and hold circuit that charges a capacitor to the peak video-pulse voltage and holds the charge until the next pulse, at which time the capacitor is discharged and recharged to the new pulse level. With moderate low-pass filtering, this gives the dc error voltage output to the servo amplifier to correct the antenna position.

The three-channel amplitude-comparison monopulse tracking radar is the most commonly used monopulse system. However, the three signals may sometimes be combined in other ways to perform with a two-channel receiver system (as described later in this section) used in some current surface-to-air missile (SAM) systems.

Monopulse-Antenna Feed Techniques. Monopulse-radar feeds may have any of a variety of configurations. Single apertures are also employed by use of higher-order waveguide modes to extract angle-error-sensing difference signals. There are many tradeoffs in feed design because optimum sum and difference signals, low sidelobe levels, selectable polarization capability, and simplicity cannot all be fully satisfied simultaneously. The term *simplicity* refers not only to cost savings but also to the use of noncomplex circuitry, which is necessary to provide a broadband system with good boresight stability to meet precision-tracking requirements. (*Boresight* is the electrical axis of the antenna or the angular location of a signal source within the antenna beam at which the angle-error-detector outputs go to zero.)

Some of the typical monopulse feeds are described to show the basic relations and tradeoffs involved in the various performance factors and how the more important factors can be optimized by a feed configuration but at the price of lower performance in other areas.[4] Many new techniques have been added since the original four-horn square feed in order to provide good or excellent performance in all desired feed characteristics in a well-designed monopulse radar.

The original four-horn square monopulse feed is inefficient because the optimum feed size aperture for the difference signals is approximately twice the optimum size for the sum signal.[5] Consequently, an intermediate size is typically used with a significant compromise for both sum and difference signals. The optimum four-horn square feed, which is subject to this compromise, described in Sherman,[1] is based on minimizing the angle error caused by receiver thermal noise. However, if sidelobes are a prime consideration, a somewhat different feed size may be desired.

The limitation of the four-horn squared feed is that the sum- and difference-signal *E* fields cannot be controlled independently. If independent control could be provided, the *ideal* would be approximately as described in Figure 9.4, with twice the dimension for the difference signals in the plane of error sensing than for the sum signal.[5]

A technique used by the MIT Lincoln Laboratory to approach the ideal is a 12-horn feed (Figure 9.5). The overall feed, as illustrated, is divided into small parts, and the microwave circuitry selects the portions necessary for the sum and difference signals to approach the ideal. One disadvantage is that this feed requires a very complex microwave circuit. Also, the divided four-horn portions of the feed are each four element arrays that generate large feed sidelobes in the *H*-plane because of the double-peak *E* field. Another consideration is that the 12-horn feed is not practical for focal-point-fed parabolas or reflectarrays because of its size. A focal-point feed is usually small to produce a broad pattern and must be compact to avoid blockage of the antenna aperture. In some cases, the small optimum size required is below waveguide cutoff, and dielectric loading of the horn apertures becomes necessary to avoid cutoff.

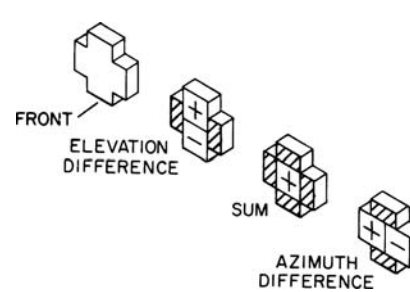

FIGURE 9.4 Approximately ideal feed-aperture *E*-field distribution for sum and difference signals

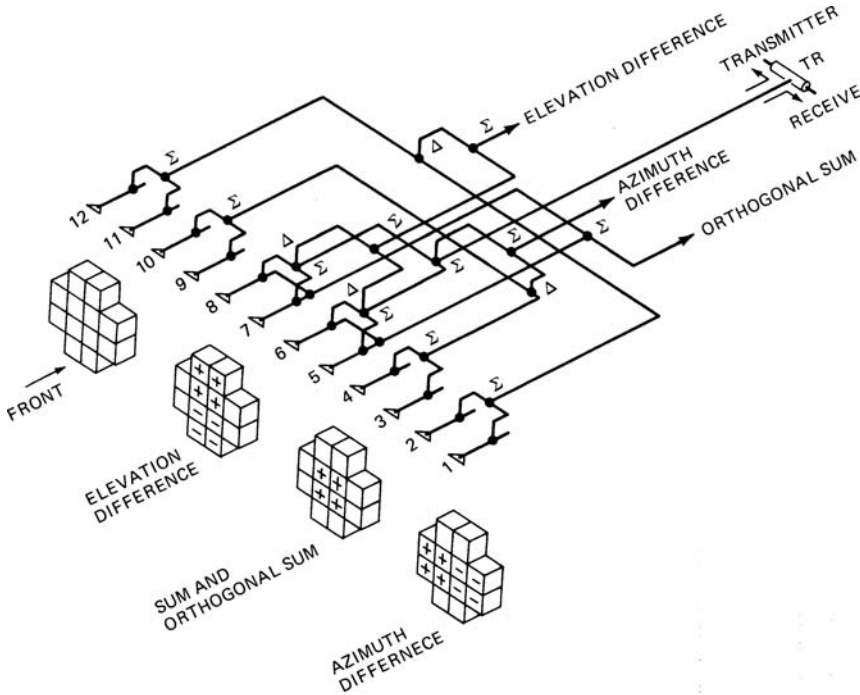

FIGURE 9.5 Twelve-horn feed

A practical approach to monopulse feed design uses higher-order waveguide modes rather than multiple horns for independent control of sum- and difference-signal *E* fields. This allows much greater simplicity and flexibility. A triple-mode two-horn feed used by RCA[5,6] retracts the *E*-plane septa to allow both the TE_{10} and TE_{30} modes to be excited and propagate in the double-width septumless region, as illustrated in Figure 9.6. At the septum, the double-humped *E* field is represented by the combined TE_{10} and TE_{30} modes subtracting at the center and adding at the TE_{30}-mode outer peaks. However, because the two modes propagate at different velocities, a point is reached farther down the double-width guide where the two modes add in the center and subtract at the outer humps of the TE_{30} mode. The result is a sum-signal *E* field concentrated, as desired, toward the center of the feed aperture.

This shaping of the sum-signal *E* field is accomplished independently of the difference-signal *E* field. The difference signal is two TE_{10}-mode signals, side by side, arriving at the septum of Figure 9.6 out of phase. At the septum, it becomes the TE_{20} mode, which propagates to the horn aperture and uses the full width of the horn as desired. The TE_{20} mode has zero *E* field in the center of the waveguide where the septum is located and is unaffected by the septum.

A further step in feed development is the four-horn triple-mode feed illustrated in Figure 9.7.[5] This feed uses the same approach as described above but with the addition of a top and bottom horn. This allows the *E*-plane difference signal to couple to all four horns and uses the full height of the feed. The sum signal uses only the center two horns to limit its *E* field in the *E*-plane as desired for the ideal field shaping.

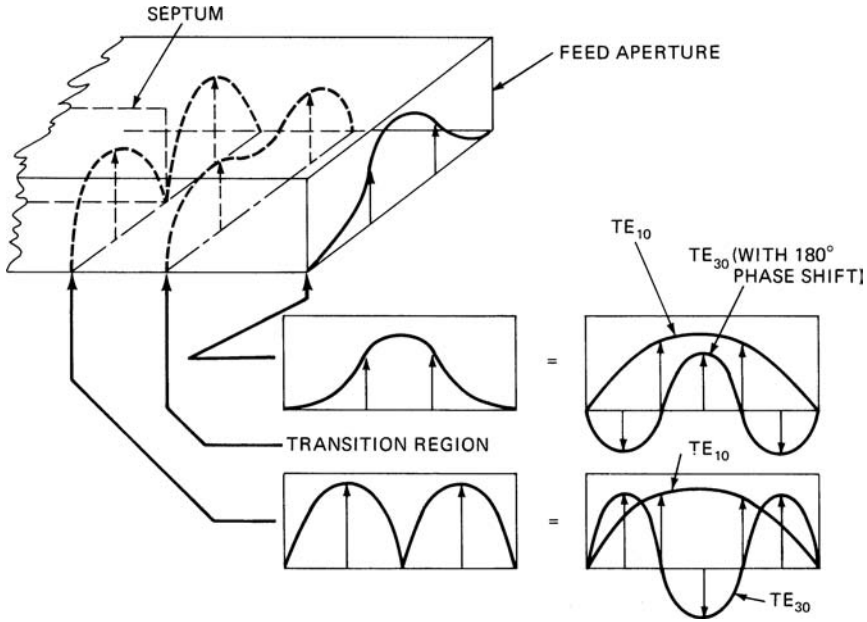

FIGURE 9.6 Use of retracted septum to shape the sum-signal *E* field

The use of smaller top and bottom horns is a simpler method of concentrating the *E*-field toward the center of the feed, where the full horn width is not needed.

The feeds described thus far are for linear-polarization operation. When circular polarization is needed in a paraboloid-type antenna, square or circular cross-section horn throats are used. The vertical and horizontal components from each horn are

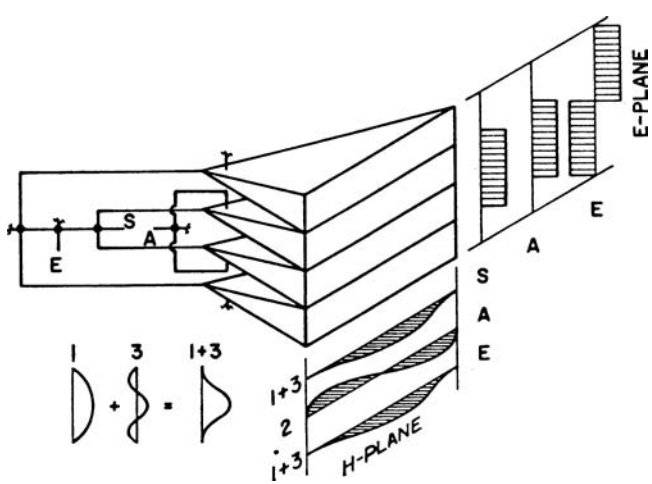

FIGURE 9.7 Four-horn triple-mode feed (*after P. W. Hannan*[5] © *IEEE 1961*)

separated and comparators provided for each polarization. The sum and difference signals from the comparators are combined with 90° relative phase to obtain circular polarization. Use of the previously described feeds for circular polarization would require the waveguide circuitry to be prohibitively complex. Consequently, a five-horn feed has been used as illustrated in Figure 9.8.

The five-horn feed is selected because of the simplicity of the comparator that requires only two magic (or hybrid) T's for each polarization. The sum and difference signals are provided for the two linear-polarization components and, in an AN/FPQ-6 radar, are combined in a waveguide switch for selecting polarization. The switch selects either the vertical or the horizontal input component or combines them with a 90° relative phase for circular polarization. This feed does not provide optimum sum- and difference-signal E fields because the sum horn occupies space desired for the difference signals. Generally, an undersized sum-signal horn is used as a compromise. However, the five-horn feed is a practical choice between complexity and efficiency. It has been used in several instrumentation radars including the AN/FPQ-6, AN/FPQ-10, AN/TPQ-18, andAN/MPS-36[7,8] and in the AN/TPQ-27 tactical precision-tracking radar.[9]

The multimode feed technique can be expanded to other higher-order modes for error sensing and E-field shaping.[10,11,12] The difference signals are contained in unsymmetrical modes such as the TE_{20} mode for H-plane error sensing and combined TE_{11} and TM_{11} modes for E-plane error sensing. These modes provide the difference signals, and no comparators are used.[10] Generally, mode coupling devices can give good performance in separating the symmetrical and unsymmetrical modes without significant cross-coupling problems.

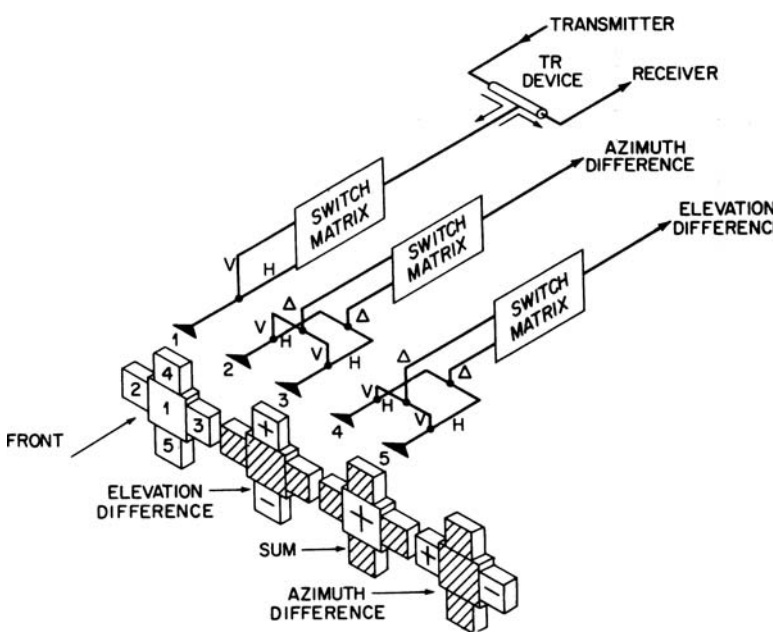

FIGURE 9.8 Five-horn feed with coupling to both linear-polarization components, which are combined by the switch matrix to select horizontal, vertical, or circular polarization

Multiband monopulse feed configurations are practical and in use in several systems. A simple example is a combined X-band and K_a-band monopulse paraboloid antenna radar. Separate conventional feeds are used for each band, with the K_a-band feed as a Cassegrain feed and the X-band feed at the focal point.[13] The Cassegrain subdish is a hyperbolic-shaped highly efficient grid of wires reflective to parallel polarization and transparent to orthogonal polarization. It is oriented to be transparent to the X-band focal-point feed behind it and reflective to the orthogonally polarized K_a-band feed extending from the vertex of the paraboloid.

Monopulse feed horns at different microwave frequencies can also be combined with concentric feed horns. The multiband feed clusters will sacrifice efficiency but can satisfy multiband requirements in a single antenna.

AGC (Automatic Gain Control). To maintain a stable closed-loop servosystem for angle tracking, the radar must maintain essentially constant loop gain independent of target echo size and range. The problem is that monopulse difference signals from the antenna are proportional to both the angle displacement of the target from the antenna axis and the echo signal amplitude. For a given tracking error, the error voltage would change with echo amplitude and target range causing a corresponding change in loop gain.

AGC is used to remove the angle-error-detector-output dependence on echo amplitude and retain constant tracking loop gain. A typical AGC technique is illustrated in Figure 9.9 for a one-angle coordinate tracking system. The AGC system detects the peak voltage of the sum signal and provides a negative dc voltage proportional to the peak signal voltage. The negative voltage is fed to the IF amplifier stage, where it is used to decrease gain as the signal increases. A high gain in the AGC loop is equivalent to dividing the IF output by a factor proportional to its amplitude.

In a three-channel monopulse radar, all three channels are controlled by the AGC voltage, which effectively performs a division by the magnitude of the sum signal or echo amplitude. Conventional AGC essentially holds constant gain during the pulse repetition interval. Also, the AGC of the sum channel normalizes the sum echo pulse amplitude to similarly maintain a stable range-tracking servo loop.

The angle-error detector, assumed to be a produce detector, has an output

$$|e| = k\frac{\Delta\Sigma}{|\Sigma||\Sigma|}\cos\theta \tag{9.2}$$

where $|e|$ is the magnitude of the angle-error voltage. Phases are adjusted to provide 0° or 180° on a point-source target. The resultant is

$$|e| = \pm k\frac{\Delta}{|\Sigma|} \tag{9.3}$$

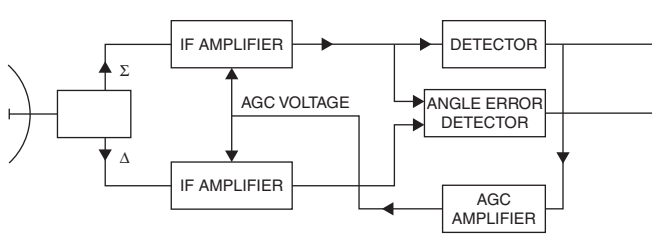

FIGURE 9.9 AGC in monopulse tracking

Complex targets can cause other phase relations as a part of the angle scintillation phenomenon.[1] The above error voltage, proportional to the ratio of the difference signal divided by the sum signal, is the desired angle-error-detector output, giving a constant angle error sensitivity.[1]

With limited AGC bandwidth, some rapid signal fluctuations modulate $|e|$ but the long-time-average angle sensitivity is constant. These fluctuations are largely from rapid changes in target reflectivity, $\sigma(t)$, that are from target amplitude scintillation. The random modulation of $|e|$ causes an additional angle noise component that affects the choice of AGC bandwidth.

The AGC performance in conical-scan radars provides similar constant angle error sensitivity. One major limitation in conical-scan radars is that the AGC bandwidth must be sufficiently lower than the scan frequency to prevent the AGC from removing the modulation containing the angle error information.

Phase-Comparison Monopulse. A second monopulse technique is the use of multiple antennas with overlapping (nonsquinted) beams pointed at the target. Interpolating target angles within the beam is accomplished, as shown in Figure 9.10, by comparing the phase of the signals from the antennas (for simplicity a single-coordinate tracker is described). If the target were on the antenna boresight axis, the outputs of each

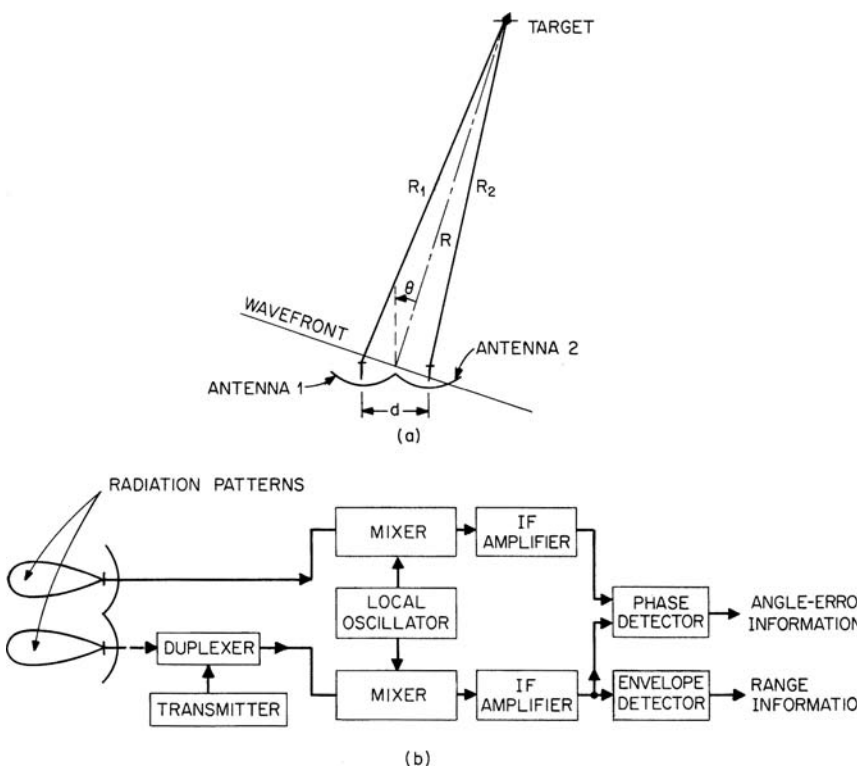

FIGURE 9.10 (*a*) Wavefront phase relationships in a phase comparison monopulse radar and (*b*) block diagram of a phase comparison monopulse radar (one angle coordinate)

individual aperture would be in phase. As the target moves off axis in either direction, there is a change in relative phase. The amplitudes of the signals in each aperture are the same so that the output of the angle-error phase detector is determined by the relative phase (see Figure 9.11). The phase-detector circuit is adjusted with a 90° phase shift on one channel to give zero output when the target is on axis and an output increasing with increasing angular displacement of the target with a polarity corresponding to the direction of error.

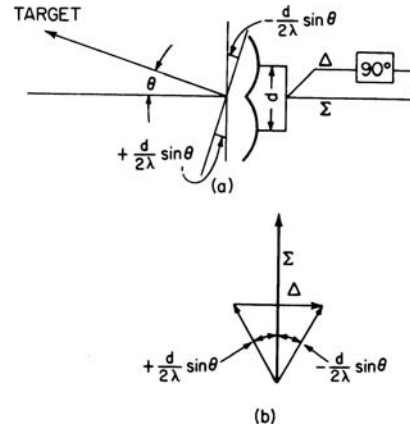

FIGURE 9.11 (*a*) RF phase-comparison monopulse system with sum and difference outputs and (*b*) vector diagram of the sum and difference signals

Typical flat-face corporate-fed phased arrays compare the output of halves of the aperture and fall into the class of phase-comparison monopulse. However, the basic signal processing of amplitude- and phase-comparison monopulse is similar, but the control of amplitude distribution across an array aperture for the sum and difference signals maintains efficiency and lower sidelobes.

Figure 9.10 shows the antenna and receiver for one angular-coordinate tracking by phase comparison monopulse. Any phase shifts occurring in the mixer and IF amplifier stages causes a shift in the boresight of the system. The disadvantages of phase-comparison monopulse with separate apertures compared with amplitude-comparison monopulse are the relative difficulty in maintaining a highly stable boresight and the difficulty in providing the desired antenna illumination taper for both sum and difference signals. The longer paths from the antenna outputs to the comparator circuitry make the phase-comparison system more susceptible to boresight change due to mechanical loading (sag), differential heating, etc.

A technique giving greater boresight stability combines the two antenna outputs at RF with passive circuitry to yield sum and difference signals, as shown in Figure 9.11. These signals may then be processed like a conventional amplitude-comparison monopulse receiver. The system shown in Figure 9.11 would provide a relatively good difference-channel taper, having smoothly tapered *E*-fields on each antenna. However, a sum-signal excitation with the two antennas provides a two-humped in-phase *E*-field distribution that causes high sidelobes since it looks like a two-element array. This problem may be reduced by allowing some aperture overlap but at the price of loss of angle sensitivity and antenna gain.

Electronic Scan Phased Array Monopulse. Tracking radars dedicated to single target tracking can provide very high precision long range performance, such as the AN/FPQ-6[14,15,16] (Figure 9.1*a*) with a specified precision of 0.05 milliradian. With high power and a high gain antenna (52 dB) and special tracking techniques, they are the workhorse for precision tracking of satellites and similar tasks. However, most modern tasks require precision simultaneous tracking of multiple simultaneous targets where use of multiple single target tracking radars are not cost effective. The development of electronic scan phased array technology has resulted in versatile high precision monopulse tracking with the capability of simultaneous multitarget tracking by switching its beam to each of several targets on a pulse-to-pulse basis or by groups

of pulses. Monopulse tracking is necessary to obtain angle data on each pulse to maintain adequate data rates when sharing pulses and power among several targets. A detailed discussion of electronic scan phased arrays is given in Chapter 13; however, some characteristics of the arrays require special consideration for the angle tracking performance of tracking radars using monopulse phased array antennas.

Optical-feed Monopulse Electronic Scan Arrays. Optical-feed monopulse arrays include the lens array and reflectarray (Chapter 13) that are optically fed by a conventional monopulse feed. The AN/MPQ-39[17] (Figure 9.1*b*) is an example of an optically fed array lens with the antenna mounted on a two-axis pedestal. Typical instantaneous electronic angle coverage is ±45° to an almost ±60° cone field-of-view that may be moved by pedestal drive to center on a multitarget event or follow an event progressing to a different area. Some military systems such as the Patriot with the ±60° cone of instantaneous view is fixed on its vehicle without a pedestal and is dependent on movement of its vehicle to change the region of angular coverage as needed. The advantages of space fed arrays are

- Conventional monopulse microwave horn feeds are used.
- Array elements are available with selectable polarization of the radiated energy when fed by an optimized linear polarized monopulse feed (such as in Figure 9.7) and selectable receive-polarization as well. This avoids the typical compromise and greater complexity of a polarization-controlled monopulse feed as described in Figure 9.8.
- Electronic scan array lenses can also refocus from a transmit feed horn to an adjacent receive feed horn on reception to allow high power transmission through a simple single horn feed to simplify isolation of the receiver from the transmit power.
- Arrays allow greater flexibility to optimize amplitude distribution of the radiated energy across the array to reduce sidelobes.

Most of the electronic scan phased array disadvantages are described in Chapter 13 and include losses in the array phase shifting elements, limitation of instantaneous bandwidth with conventional phase control elements (improved with special true-time-delay phase shifting), phase quantization errors (Chapter 13) resulting from phase shifting in steps, restriction to a single rf band (multiband arrays require special techniques with major compromises), and gradual degradation of performance as the beam is scanned from the normal to the array. The quantization errors from phase shifting in steps are of concern to monopulse radar because it results in corresponding random error steps in the electronic axis of the array. As described in Chapter 13, the quantization errors are inversely proportional to the number of phase shifting elements and 2^P where P is the number of bits of phase control in each element. Consequently, the high precision tracking radars with typically 4000 to 8000 phase shifters and four or more phase shift bits have small resultant electrical axis error steps on the order of 0.1 milliradians or less. The electrical axis errors are essentially random and can be further reduced by averaging. Intentional dither of phase steps may be introduced to aid in averaging.

The optically fed technique results in feed energy spillover around the aperture; however, these resultant spillover sidelobes can be eliminated by an absorbing cone between the feed and the array aperture. The absorbing cone is observed in the AN/MPQ-39 (Figure 9.1*b*). However, cooling is also necessary and provided, as observed by the cooling coils around the absorbing cone.

Of further concern to high precision monopulse applications is drift of the electronic axis that causes variations in phase and temperature variation across the array surface that causes distortion of the lens. Significant variation of heat distribution across the array face can result from high power transmitted through the phase shifting elements as well as the electronic phase control. Consequently, where high precision tracking is required, special cooling techniques may be necessary to maintain constant temperature across the aperture.

Corporate Feed Monopulse Electronic Scan Phased Array. The corporate feed array is fed by dividing and subdividing the transmit signal through transmission lines typically to subarrays of multiple array radiating elements. This technique, although typically resulting in heavier and higher cost implementation, offers the advantage of flexibility of control of the signal paths through the array structure, as described in Chapter 13. Another advantage is the capability to transmit very high peak power without the limitations of full peak power propagating through a single transmission line. This is accomplished in the corporate feed array by placing high power amplifiers where the power divides to the subarrays, allowing the sum of the high peak power amplifier outputs to add in space to meet requirements for long-range tracking and power sharing between multiple simultaneous targets.

The parallel power amplifier configuration also provides a practical means for overcoming the narrow instantaneous bandwidth of typical phased arrays at wide scan angles. Full array instantaneous bandwidth requires equal path lengths between each array element and the target, requiring many wavelengths of phase control or the equivalent time delay in array elements at wide angle scans. However, this control has prohibitively high loss for typical phased array radiating elements; consequently, typical phased array elements provide only sufficient phase control of up to 360° or to one wavelength, limited to tolerable loss, to cause the signal from each element to arrive approximately in phase at the target. Unfortunately, this shortcut is adequate for only a narrow instantaneous bandwidth. The parallel power amplifiers, as described above, provide a low power amplifier drive stage where the high loss of the desired time delay control can be tolerated to gain wide instantaneous bandwidth, as described in Chapter 13. The time delay may be controlled similar to the diode phase shifters used in radiating elements that switch between different line lengths to adjust phase. Longer time delay transmission line could be similarly controlled by diode switching to provide the wide instantaneous bandwidth to allow, for example, use of wideband narrow pulses to provide the range resolution requirements for tracking radar applications.

Two-Channel Monopulse. Monopulse radars may be designed with fewer than the conventional three IF channels. This is accomplished, for example, by combining the sum and difference signals in two IF channels and the sum and two difference signal outputs are then individually retrieved at the output. These techniques provide some advantages in AGC or other processing techniques but at the cost of reduced SNR, reduced angle data rate, and potential for cross coupling between azimuth and elevation information.

A two-channel monopulse receiver[18] combines the sum and difference signals at RF, as shown in Figure 9.12. The microwave resolver is a mechanically rotated RF coupling loop in cylindrical waveguide. The azimuth and elevation difference signals are excited in this guide with *E*-field polarization oriented at 90°. The energy in the coupler contains both difference signals coupled as the cosine and sine of the angular position of the coupler, $\omega_s t$, where ω_s is the angular rate of rotation. The hybrid adds the combined difference signals Δ at the angular

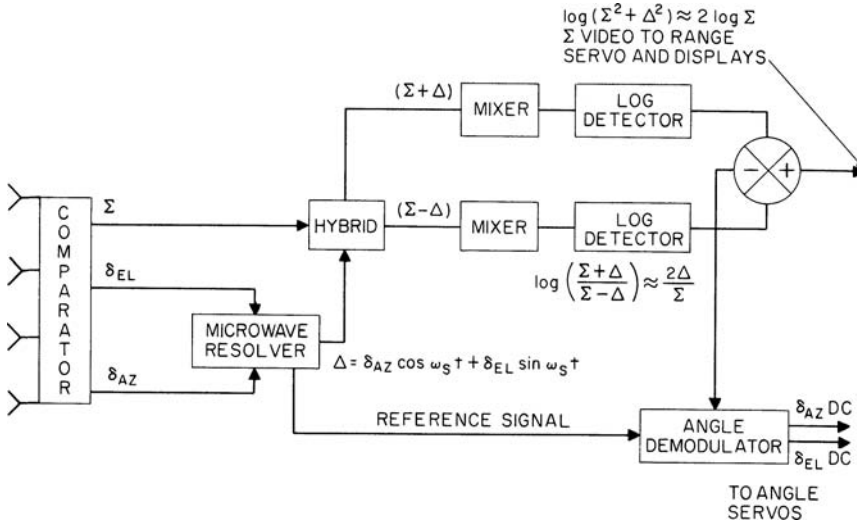

FIGURE 9.12 Block diagram of a two-channel monopulse radar system (*from R. S. Noblit*[18])

rate of rotation. The $\Sigma + \Delta$ and $\Sigma - \Delta$ outputs each look like the output of a conical-scan tracker except that their modulation function differs by 180°. In case one channel fails, the radar can be operated as a scan-on-receive-only conical-scan radar with essentially the same performance as a conical-scan radar. The advantage of two channels with opposite-sense angle-error information on one channel with respect to the other is that signal amplitude fluctuations in the received signal are canceled in the post-detection subtraction at the IF output that retrieves the angle-error information. The log IF performs essentially as an instantaneous AGC, giving the desired constant angle-error sensitivity of the difference signals normalized by the sum signal. The detected Δ information is a bipolar video where the error information is contained in the sinusoidal envelope. This signal is separated into its two components, azimuth- and elevation-error information, by an angle demodulation. The demodulator, using a reference from the drive on the rotating coupler, extracts the sine and cosine components from Δ to give the azimuth- and elevation-error signals. The modulation caused by the microwave resolver is of concern in instrumentation radar applications because it adds spectral components in the signal, complicating the possible addition of pulse doppler tracking capability to the radar.

This system provides instantaneous AGC operation with only two IF channels and operation with reduced performance in case of failure of either channel. However, there is a loss of 3-dB SNR at the receiver inputs, although this loss is partly regained by coherent addition of the Σ-signal information. The design of the microwave resolver must minimize loss through the device, and precisely matched IF channels are required to minimize cross coupling between the azimuth and elevation channels. In some modern systems, the resolver performance is improved by use of ferrite switching devices to replace the mechanical rotating coupler.

Conopulse. Conopulse (also called *scan with compensation*) is a radar tracking technique that is a combination of monopulse and conical scan.[19,20] A pair of antenna

beams is squinted in opposite directions from the antenna axis and rotated like a pair of conical-scan-radar beams. Since they exist simultaneously, monopulse information can be obtained from the pair of beams. The plane in which monopulse information is measured rotates. Consequently, elevation and azimuth information is sequential and must be separated for use in each tracking coordinate. Conopulse provides the monopulse advantage of avoiding errors caused by amplitude scintillation, and it requires only two receivers. However, it has the disadvantage of lower angle data rates and the mechanical complexity of providing and coupling to a pair of rotating antenna feedhorns.

9.3 SCANNING AND LOBING

The first technique used for radar angle tracking was to displace the antenna beam above and below the target in elevation and side to side of the target in azimuth to compare beam amplitudes similar to monopulse radar simultaneous lobing but differing by being in a time sequence. This was performed by a continuous conical beam scan, as illustrated in Figure 9.13[21] or by sequentially lobing up/down and right/left and observing the difference between amplitudes as a measure of displacement of the antenna axis from the target. The signal output for a conical-scan radar, illustrated in Figure 9.14, is typically a sinusoid amplitude modulation of the received target echo pulses. The amplitude of the modulation is a measure of the magnitude of the angle error, and the phase, relative to the scanning-beam rotation angle, indicates the portion of the error caused by each tracking axis.

The performance of scanning and lobing radar relative to the beam offset angle is described in Barton.[22] An optimum beam offset is described as a compromise between the loss of antenna gain and the increase in sensitivity to target angle displacement from the antenna axis as beam offset is increased. The optimum offset is typically chosen to provide the minimum rms angle-tracking error as affected by the signal-to-noise ratio and tracking sensitivity. Special tracking radar applications with nontypical requirements could arrive at a different optimum beam offset.

A major limitation of scanning and lobing radar is the susceptibility to target amplitude fluctuations that occur during the time the beam is moved from side to side or up and down. It is also susceptible to false modulation on signals from countermeasures. The echo fluctuations not related to antenna beam position cause false target angle-tracking errors.

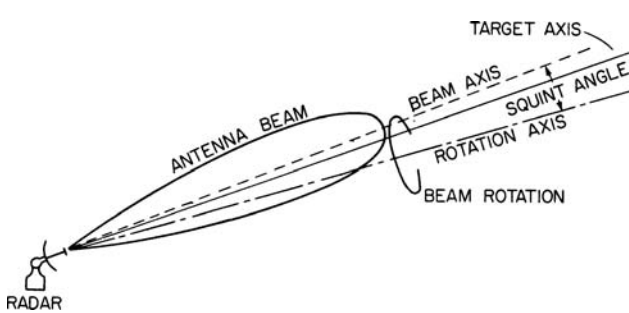

FIGURE 9.13 Conical-scan tracking

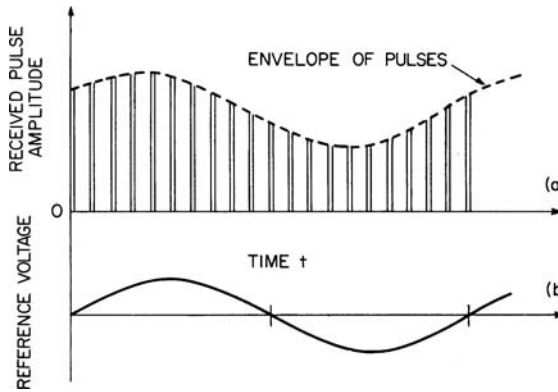

FIGURE 9.14 (*a*) Angle error information contained in the envelope of the received pulses in a conical-scan radar and (*b*) reference signal derived from the drive of the conical-scan feed

Monopulse radar was developed to provide simultaneous offset antenna beams for comparison of target echo amplitudes on a single pulse independent of echo signal amplitude fluctuations. However, few microwave devices and components were initially available, and the first monopulse systems were complex and resulted in cumbersome and inefficient antennas. At present, modern monopulse radars, as described in Section 9.2, provide highly stable and efficient antennas with high precision performance and have generally displaced scanning and lobing tracking radars for meeting the increasing demands for high precision and high data rate of angle information on each pulse. However, special radar tracking requirements may exist where a practical implementation of conical scan or lobing tracking radar may more effectively provide adequate performance.

9.4 SERVOSYSTEMS FOR TRACKING RADAR

The servosystem of a tracking radar is the subsystem of the radar that receives as its input the tracking-error voltage and performs the task of moving the antenna beam in a direction that will reduce to zero the alignment error between the antenna axis and the target. For two-axis tracking with a mechanical-type antenna pedestal, there are typically separate axes of rotation for azimuth and elevation and separate servosystems to move the antenna about each axis. A conventional servosystem is composed of amplifiers, filters, and a motor that moves the antenna in a direction to maintain the antenna axis on the target. Range tracking is accomplished by a similar system to maintain range gates centered on the received echo pulses. This may be accomplished by analog techniques or by digital-counter registers that retain numbers corresponding to target range to provide a closed range-tracking loop digitally.

Servosystems may use hydraulic-drive motors, conventional electric motors geared down to drive the antenna, or direct-drive electric motors where the antenna mechanical axis shaft is part of the armature, and the motor field is built into the support case. The direct drive is heavier for a given horsepower but eliminates

gear backlash. Backlash may also be reduced with conventional motors by duplicate parallel drives with a small residual opposing torque when near zero angle rate. Amplifier gain and filter characteristics as well as motor torque and inertia determine the velocity and acceleration capability or the ability to follow the higher-order motion of the target.

It is desired that the antenna beam follow the center of the target as closely as possible, which implies that the servosystem should be capable of moving the antenna quickly. The combined velocity and acceleration characteristics of a servosystem can be described by the frequency response of the tracking loop, which acts essentially like a low-pass filter. Increasing the bandwidth increases the quickness of the servosystem and its ability to follow a strong, steady signal closely. However, a typical target causes scintillation of the echo signal, giving erroneous error-detector outputs, and at long range, the echo is weak, allowing receiver noise to cause additional random fluctuations on the error detector output. Consequently, a wide servo bandwidth, which reduces lag errors, allows the noise to cause greater erroneous motions of the tracking system. Therefore, for best overall performance, it is necessary to limit the servo bandwidth to the minimum necessary to maintain a reasonably small tracking-lag error. There is an optimum bandwidth that may be chosen to minimize the amplitude of the total erroneous outputs including both tracking lag and random noise, depending upon the target, its trajectory, and other radar parameters.

The optimum bandwidth for angle tracking is range-dependent. A target with typical velocity at long range has low angle rates and a low SNR, and a narrower servo passband will follow the target with reasonably small tracking lag while minimizing the response to receiver thermal noise. At close range, the signal is strong, overriding receiver noise, but target angle scintillation errors proportional to the angular span of the target are large. A wider servo bandwidth is needed at close range to keep tracking lag within reasonable values, but it must not be wider than necessary or the target angle scintillation errors, which increase inversely proportional to target range, may become excessive.

The low-pass closed-loop characteristic of a servosystem is unity at zero frequency, typically remaining near this value up to a frequency near the low-pass cutoff, where it may peak up to higher gain, as shown in Figure 9.15*a*. The peaking is an indication of system instability but is allowed to be as high as tolerable, typically to about 3 dB above unity gain to obtain maximum bandwidth for a given servomotor drive system. System A in Figure 9.15*a* is a case of excessive peaking of about 8 dB. The effect of the peaking is observed by applying a step error input to the servosystem. The peaking of the low-pass characteristic results in an overshoot when the antenna axis moves to align with the target. High peaking causes a large overshoot and a return to the target with additional overshoot. In the extreme (as in system A shown in Figure 9.15*b*), the antenna zeros in on the target with a damped oscillation. An optimum system compromise between speed of response and overshoot, as in system B, allows the antenna to make a small overshoot with reasonably rapid exponential movement back to the target. This corresponds to about 1.4 dB peaking of the closed-loop low-pass characteristic.

The resonant frequency of the antenna and servosystem structure (including the structure foundation, which is a critical item) must be kept well above the bandwidth of the servosystem, otherwise the system can oscillate at the resonant frequency. A factor of at least 10 is desirable for the ratio of system resonance frequency to servo bandwidth. High resonant frequency is difficult to obtain with a large antenna, such as the AN/FPQ-6 radar with a 29-ft dish, because of the large mass of the system.

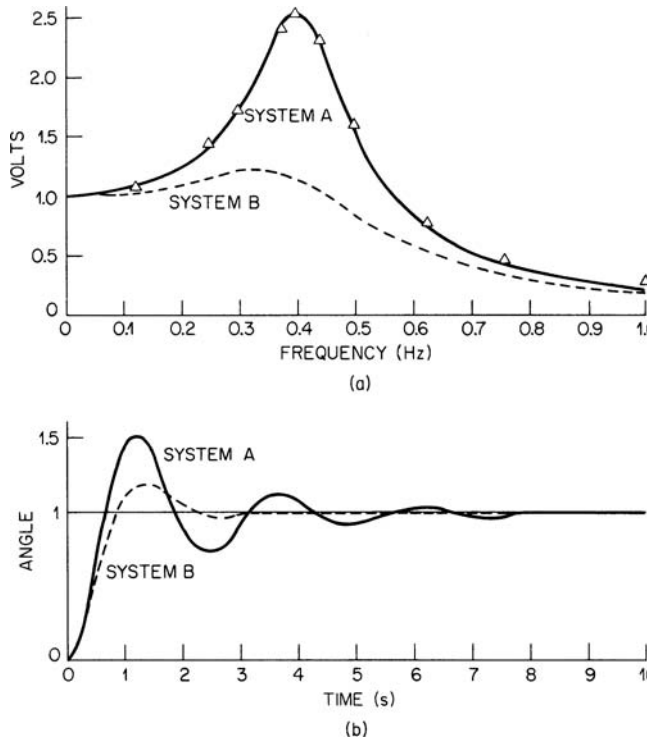

FIGURE 9.15 (*a*) Closed-loop frequency-response characteristics of two servosystems and (*b*) their corresponding time response to a step input

The ratio was pushed to a very minimum of about 3 to obtain servosystem bandwidth of the specified 3.5 Hz. A smaller radar with a 12-ft dish, for example, can provide a servosystem bandwidth up to 7 or 8 Hz with conventional design.

Locke[23] describes methods for calculating angle tracking lag for a given target trajectory versus time and set of servosystem characteristics. Range tracking lags may be similarly calculated, but with typical inertialess electronic tracking systems, tracking lags are usually negligible.

Electronically steerable arrays provide a means for inertialess angle tracking. However, because of this capability, the system can track multiple targets by rapidly switching from one to another rather than continuously tracking a single target.

The tracker simply places its beam at the location where the target is expected, corrects for the pointing error by converting error voltages (with known angle-error sensitivity) to units of angle, and moves to the next target. The system determines where the target was and, from calculations of target velocity and acceleration, predicts where it should be the next time the beam looks at the target. The lag error, in this case, is dependent on many factors, including the accuracy of the value of angle sensitivity used to convert error voltages to angular error, the size of the previous tracking error, and the time interval between looks.

9.5 TARGET ACQUISITION AND RANGE TRACKING

Range tracking is accomplished by continuously measuring the time delay between the transmission of an RF pulse and the echo signal returned from the target, and converting the roundtrip delay to units of distance. The range measurement is the most precise position-coordinate measurement of the radar; typically, with high SNR, it can be within a few meters at hundreds-of-miles range. Range tracking usually provides the major means for discriminating the desired target from other targets (although doppler frequency and angle discrimination are also used) by performing range gating (time gating) to eliminate the echo of other targets at different ranges from the error-detector outputs. The range-tracking circuitry is also used for acquiring a desired target. Range tracking requires not only that the time of travel of the pulse to and from the target be measured but also that the return is identified as a target rather than noise and a range-time history of the target be maintained.

Although this discussion is for typical pulse-type tracking radars, range measurement may also be performed with CW radars using FM-CW, a frequency-modulated CW that is typically a linear-ramp FM. The target range is determined by the range-related frequency difference between the echo-frequency ramp and the frequency of the ramp being transmitted. The performance of FM-CW systems, with consideration of the doppler effect, is described in Sherman.[1]

Acquisition. The first function of the range tracker is acquisition of a desired target. Although this is not a tracking operation, it is a necessary first step before range tracking or angle tracking may take place in a typical radar. Some knowledge of target angular location is necessary for pencil-beam tracking radars to point their typically narrow antenna beams in the direction of the target. This information, called *designation data,* may be provided by surveillance radar or some other source. It may be sufficiently accurate to place the pencil beam on the target, or it may require the tracker to scan a larger region of uncertainty. The range-tracking portion of the radar has the advantage of seeing all targets within the beam from close range out to the maximum range of the radar. It typically breaks this range into small increments, each of which may be simultaneously examined for the presence of a target. When beam scanning is necessary, the range tracker examines the increments simultaneously for short periods, such as 0.1 s, makes its decision about the presence of a target, and allows the beam to move to a new location if no target is present. This process is typically continuous for mechanical-type trackers that move the beam slowly enough that a target will remain well within the beam for the short examination period of the range increments.

Target acquisition involves consideration of the *S/N* threshold and integration time needed to accomplish a given probability of detection with a given false-alarm rate similar to surveillance radar. However, high false-alarm rates, as compared with values used for surveillance radars, are used because the operator knows that the target is present, and operator fatigue from false alarms when waiting for a target is not involved. Optimum false-alarm rates are selected on the basis of performance of electronic circuits that observe each range interval to determine which interval has the target echo.

A typical technique is to set a voltage threshold sufficiently high to prevent most noise peaks from crossing the threshold but sufficiently low that a weak signal may cross. An observation is made after each transmitter pulse as to whether, in the range interval being examined, the threshold has been crossed. The integration time allows the radar to make this observation several times before deciding if there is a target present.

The major difference between noise and a target echo is that noise spikes exceeding the threshold are random, but if a target is present, the threshold crossings are more regular. One typical system simply counts the number of threshold crossings over the integration period, and if crossings occur for more than half the number of times that the radar has transmitted, a target is indicated as being present. If the radar pulse repetition frequency is 300 Hz and the integration time is 0.1 s, the radar will observe 30 threshold crossings if there is a strong and steady target. However, because the echo from a weak target combined with noise may not always cross the threshold, a limit may be set, such as 15 crossings, that must occur during the integration period for a decision that a target is present. For example, performance on a non-scintillating target has a 90% probability of detection at a 2.5 dB-per-pulse SNR and a false alarm probability of 10^{-5}. The AN/FPS-16 and AN/FPQ-6 instrumentation radars use these detection parameters with 10 contiguous range gates of 1000 yd each for acquisition. The 10 gates give coverage of a 5-nmi range interval at the range where the target is expected, possibly from coarse range designation from search radar.

Range Tracking. Once a target is acquired in range, it is desirable to follow the target in the range coordinate to provide distance information or slant range to the target. Appropriate timing pulses provide range gating so the angle-tracking circuits and AGC circuits look at only the short range interval, or time interval, when the desired echo pulse is expected. The range tracking operation is performed by closed-loop tracking similar to the angle tracker. Error in centering the range gate on the target echo pulse is sensed, error voltages are generated, and circuitry is provided to respond to the error voltage by causing the gate to move in a direction to recenter on the target echo pulse.

The range-tracking error may be sensed in many ways. The most commonly used method is the early- and late-gate technique (see Figure 9.16). These gates are timed so that the early gate opens at the beginning of the main range gate and closes at the center of the main gate. The late gate opens at the center and closes at the end of the main range gate. The early and late gates each allow the target video to charge capacitors during the time when the gates are open. The capacitors act as integrators. The early-gate capacitor charges to a voltage proportional to the area of the first half of the target video pulse, and the late-gate capacitor charges negatively proportionally to the late half of the target video. When the gates are properly centered about a symmetrical video pulse, the capacitors are equally charged. Summing their charge voltages yields a zero output.

When the gates are not centered about the target video, so that the early gate extends past the center of the target video, the early-gate capacitor charged positively receives a greater charge. The late gate sees only a small portion of the pulse, resulting in a smaller negative charge. Summing the capacitor voltages results in a negative output. Over a range of errors of approximately ± 1/4 of the target-video pulse width, the voltage output is essentially a linear function of timing error and of a polarity corresponding to the direction of error. During acquisition, the target is centered in the 1000 yd acquisition gate by range-tracking techniques described as follows, and the gate is reduced to approximately the width of the radar transmit pulse for normal tracking.

Many radar range-tracking systems use high speed sampling circuitry to take three to five samples in the vicinity of the echo video pulse. The amplitudes of the samples on the leading and lagging halves of the pulse are compared for range-error sensing similar to the comparison of amplitudes in the early-late-gates range tracker.

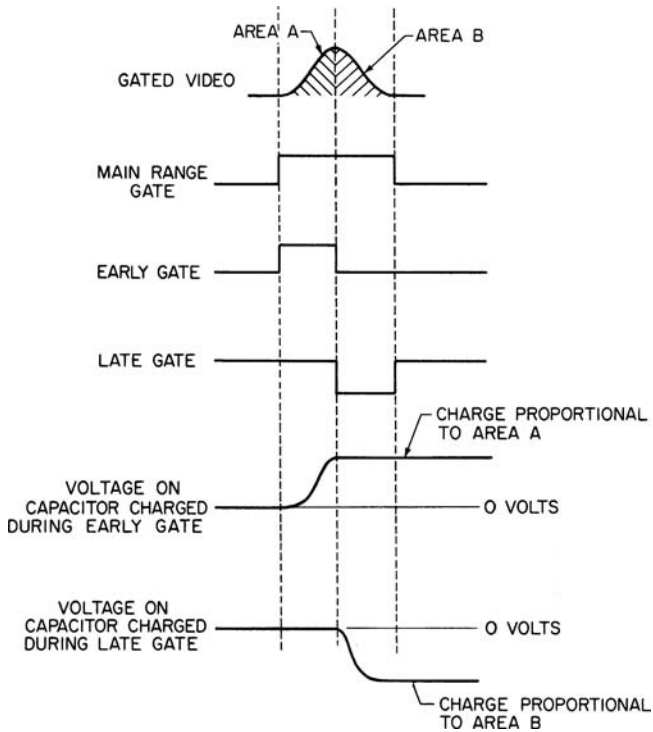

FIGURE 9.16 Early- and late-gate range-error-sensing circuit

In some cases, leading- or lagging-edge range tracking is desired. This has been accomplished in some applications by simply adding a bias to move the error-sensing gates either to lead or lag the center of the target. This provides some rejection by the gates of undesired returns that might occur near the target, such as the echoes from other nearby targets. Threshold devices are also used as leading- or lagging-edge trackers by observing when the target video exceeds a given threshold level. The point of crossing the threshold is used to trigger gating circuits to read out a target range from timing devices or to generate a synthetic target pulse.

The range-tracking loop is closed by using the range-error-detector output to reposition range gates and correct range readout. One technique uses a high-speed digital counter driven by a stable oscillator. The counter is reset to zero at the time of the transmit pulse. Target range is represented by a number stored in a digital register, as shown in Figure 9.17. A coincidence circuit senses when the digital counter reaches the number in the range register and generates the range gate, as indicated in the block diagram shown in Figure 9.18. A range error sensed by the range error detector results in an error voltage that drives a voltage-controlled variable-frequency oscillator to increase or decrease the count in the range register, depending on the polarity of the error voltage. This changes the number in the range register toward the value corresponding to the range of the target. Range readout is accomplished by reading the number in the register, where, for example, each bit may correspond to a 2-yd range step.

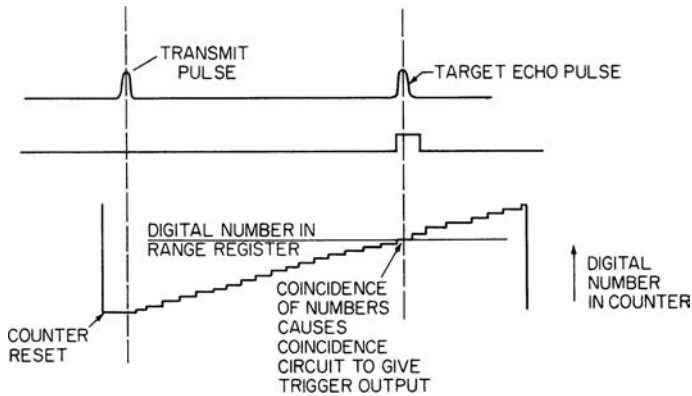

FIGURE 9.17 Digital range tracker operation

Another technique is to use a pair of oscillators—one controlling the transmitter trigger and the other controlling the range gate.[24] The range rate is controlled by the beat frequency between the oscillators, where one is frequency-controlled by the range

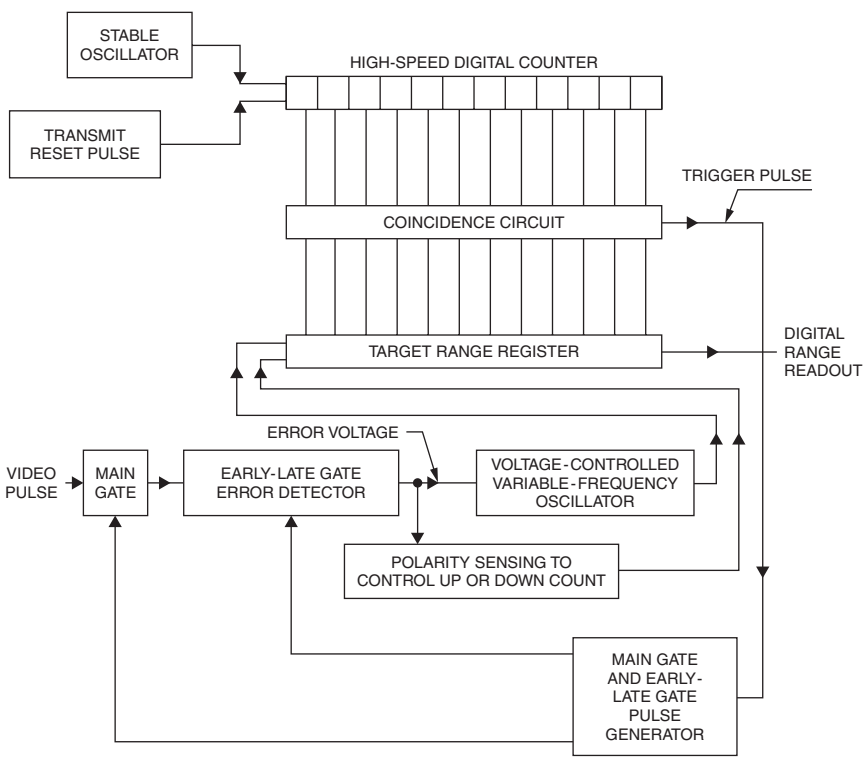

FIGURE 9.18 Block diagram of a digital range tracker

error-detector-output voltage. The beat frequency is a small fraction of one Hz and is better visualized as a phase rate between the transmit pulse cycle and cycle of the range gate. The changing phase causes the range gate to follow a moving target.

The electronic range tracker is inertialess, allowing any desired slew speed, and provides flexibility for conveniently generating acquisition gates for automatic-detection circuitry as well as transmitter trigger and pre-trigger pulses. Tracking bandwidth is usually limited to that necessary for tracking to minimize loss of track to false targets and countermeasures. Many other electronic range-tracking techniques also offering most of these advantages are used.[22]

***n*th-Time-Around Tracking.** To extend unambiguous range by reducing the PRF increases the acquisition time and reduces the data rate. A solution to this problem is called *nth-time-around tracking,* which avoids transmitting at the time that an echo is expected to arrive and can resolve the range ambiguity. This allows the radar to operate at high PRF and track unambiguously to long ranges where several pulses may be propagating in space to and from the target. The technique is useful only when a target is being tracked. During acquisition, the radar must look at the region between transmitter pulses, and upon initial acquisition, it closes the range- and angle-tracking loops without resolving the range ambiguity. The next step is to find which range interval, or between which pair of transmit pulses, the target is located. The zone n is determined by coding a transmit pulse and counting how many pulses return before the coded pulse returns.

Instrumentation radars provide *n*th-time-around tracking capability because beacons are used on rockets and space vehicles to provide sufficient signal level at very long ranges.

To prevent the target echo from being blanked by a transmit pulse, it is necessary to sense when the target is approaching an interference region and shift the region. This is accomplished by changing the PRF or alternately delaying groups of pulses equal to the number of pulses in propagation. This can be performed automatically to provide an optimum PRF shift or to alternately delay pulse groups of the correct number of pulses.

9.6 SPECIAL MONOPULSE TECHNIQUES

Dual-Band Monopulse. Dual-band monopulse can be efficiently accommodated on a single antenna to combine the complementary features of two RF bands.[13,25] A useful combination of bands is X band (9 GHz) and K_a band (35 GHz). The X-band operation provides the expected microwave performance of good radar range and precise tracking. Its weakness is the low-angle multipath region and the availability of electronic countermeasures in the band. The K_a band, although atmospheric- and rain-attenuation-limited, provides much greater tracking precision in the low-angle multipath region and a second and more difficult band that the electronic-countermeasures techniques must cover.

A Naval Research Laboratory system called TRAKX (Tracking Radar At K_a and X bands) was designed for instrumentation radar applications for missile and training ranges.[13] Its purpose was to add precision tracking on targets, essentially to "splash" and provide precision tracking at K_a band in an environment of X-band countermeasure experiments.

A similar X- and K_a-band system was developed by Hollandse Signaalapparaten of the Netherlands for tactical application. The land-based version called FLY-CATCHER is part of a mobile anti-air-warfare system.[25] Another version, GOAL-KEEPER, is for a shipboard anti-air-warfare application for the fire control of Gatling guns.[26] Both systems take full advantage of the two bands to provide precision tracking in multipath and electronic-countermeasures environments.

Mirror-Scanned Antenna (Inverse Cassegrain). An antenna technique that uses a movable RF mirror for scanning the beam, called a *mirror-scanned antenna* or *inverse Cassegrain,* provides useful applications to monopulse radar. The technique uses a radome-supported wire-grid paraboloid that reflects parallel-polarized feed energy. The beam, polarized parallel to the grid, is collimated by the paraboloid and is reflected by a flat moveable polarization rotating mirror. The basic polarization rotating mirror is a flat metal surface with a grid of wires located a quarter wavelength above the metal surface and oriented at 45° relative to the RF energy reflected from the paraboloid. The RF energy may be visualized as being composed of a component parallel to and reflecting from the grid and a component perpendicular to and passing through the grid to reflect from the metal mirror surface below. By traveling the quarter wavespace twice, this component is shifted by 180° in phase. When added to the reflection from the grid, it results in a 90° change in polarization. The total reflected energy from the mirror rotated by 90° will efficiently pass through the wire-grid paraboloid. The advantages are as follows: (1) The mirror and its drive mechanism are the only moving parts for beam movement. The feed and radome-supported paraboloid remain fixed. (2) The beam movement is by specular reflection, twice the angle of the mirror tilt. This provides a compact structure for a given angle coverage requirement. (3) The normally lightweight mirror and the 2:1 beam displacement versus mirror tilt allow reduced size and very rapid beam scan with low servo drive power.

The compactness and lightness are particularly attractive for airborne applications such as the Thompson-CSF Agave radar in the Super Entendards, which determines target range and designation data for the Exocet missile. It is a compact monopulse roll- and pitch-stabilized radar with 140° azimuth and 60° elevation scan.[27] The Israeli Elta subsidiary of Israeli Aircraft Industries also developed an airborne tracking radar using this antenna technology for air-to-air combat and ground weapon delivery.[28]

A ground- or shipboard-based experimental mirror antenna system concept was developed with dual-band monopulse capability (3.0 GHz and 9.3 GHz bands). The objective included high-speed beam movement for high-data-rate 3D surveillance and multitarget precision tracking.[29] Dual-band polarization-twist mirror design was accomplished with a two-layer mirror grid configuration.[30]

On-Axis Tracking. The best radar tracking performance is usually accomplished when the target is essentially on the radar antenna axis. Therefore, for maximum precision tracking, it is desirable to minimize lag and other error sources affecting the beam pointing. A technique called *on-axis tracking* was developed to minimize radar axis deviation from the target by prediction and optimum filtering within the tracking loop.[8,31] The technique is particularly effective when the target trajectory is known approximately, such as when tracking satellites in orbit or a ballistic target. A computer in the tracking loop can cause the radar to follow an estimated set of orbital parameters, for example. It also performs optimum filtering of radar angle-error-detector output to generate an error trend from which it can update the assumed set

of orbital parameters to correct the radar beam movement to update the original set of orbital parameters, and by this means, the radar antenna axis can be held on target with minimum error.

Improved tracking can also be provided on other targets where the approximate trajectory can be anticipated. However, performance of on-axis tracking is limited when tracking targets with unanticipated maneuvers.

9.7 SOURCES OF ERROR

There are many sources of error in radar-tracking performance. Fortunately, most are insignificant except for very high-precision tracking-radar applications such as range instrumentation, where the angle precision required may be of the order of 0.05 mrad (mrad, or milliradian, is one thousandth of a radial, or the angle subtended by 1-m cross-range at 1000-m range). Many sources of error can be avoided or reduced by radar design or modification of the tracking geometry. Cost is a major factor in providing high-precision-tracking capability. Therefore, it is important to know how much error can be tolerated, which sources of error affect the application, and what is the most cost-effective means to satisfy the accuracy requirements.

Because tracking radars track targets not only in angle but also in range and sometimes in doppler, the errors in each of these target parameters must be considered on most error budgets. The rest of this chapter will provide a guide for determining the significant error sources and their magnitudes.

It is important to recognize what the actual radar information output is. For a mechanically moved antenna, the angle-tracking output is usually obtained from the shaft position of the elevation and azimuth antenna axes. Absolute target location (relative to earth coordinates) will include the accuracy of the survey of the antenna pedestal site.

Phased array instrumentation radar, such as the Multi-object Tracking Radar (MOTR), provide electronic beam movement over a limited sector of about $\pm 45^{o}$ to approximately $\pm 60^{o}$ plus mechanical movement of the antenna to move the coverage sector.[16–19] The output will be mechanical shaft positions locating the normal to the array plus digital angle information from the electronic beam scan for each target.

9.8 TARGET-CAUSED ERRORS (TARGET NOISE)

Radar tracking of targets is performed by use of the echo signal reflected from a target illuminated by the radar transmit pulse. This is called *skin tracking* to differentiate it from *beacon tracking,* where a beacon or a transponder transmits its signal to the radar and usually provides a stronger point-source signal. Because most targets, such as aircraft, are complex in shape, the total echo signal is composed of the vector sum of a group of superimposed echo signals from the individual parts of the target, such as the engines, propellers, fuselage, and wing edges. The motions of a target with respect to the radar causes the total echo signal to change with time, resulting in random fluctuations in the radar measurements of the parameters of the target. These fluctuations caused by the target only, excluding atmospheric effects and radar receiver noise contributions, are called *target noise.*

This discussion of target noise is based largely on aircraft, but it is generally applicable to any target, including land targets of complex shape that are large with respect to a wavelength. The major difference is in the target motion, but the discussions are sufficiently general to apply to any target situation.

The echo return from a complex target differs from that of a point source by the modulations that are produced by the change in amplitude and relative phase of the returns from the individual elements. The word *modulations* is used in plural form because five types of modulation of the echo signal that are caused by a complex target affect radars. These are amplitude modulation, phase front modulation (glint), polarization modulation, doppler modulation, and pulse time modulation (range glint). The basic mechanism by which the modulations are produced is the motion of the target, including yaw, pitch, and roll, which causes the change in relative range of the various individual elements with respect to the radar.

Although the target motions may appear small, a change in relative range of the parts of a target of only one-half wavelength (because of the two-way radar signal path) causes a full 360° change in relative phase. At X band, this is about 1.5 cm, which is small even compared with the flexure between parts of an aircraft.

The five types of modulation caused by a complex target are discussed next.

Amplitude Noise. Amplitude noise is the change in echo signal amplitude caused by a complex-shaped target, excluding the effects of changing target range. It is the most obvious of the various types of echo signal modulation by a complex-shaped target and is readily visualized as the fluctuating sum of many small vectors changing randomly in relative phase. Although it is called *noise,* it may include periodic components. Amplitude noise typically falls into a low frequency and high frequency region of interest. These categories overlap in some respects, but it is convenient to separate the noise in these two frequency ranges because they are generated by different phenomena, and they are each significant to different functions of the radar.

Low-Frequency Amplitude Noise. The low-frequency amplitude noise is the time variation of the vector sum of the echoes from all the reflecting surfaces of the target. The time variation is visualized by considering the target as a relatively rigid body with normal yaw, pitch, and roll motions. The small changes in relative range of the reflectors caused by this motion result in corresponding "random" change in the relative phases. Consequently, the vector sum fluctuates randomly. Typically, target random motion is limited to small aspect changes such that the amplitudes of the echoes from the individual reflectors vary little over a period of a few seconds, and change in relative phase is the major contributor. Exceptions are large flat surfaces with narrow reflection patterns.

An example of a target configuration is a distribution of reflecting surfaces that change in relative range with target motion. A typical pulse amplitude time function is a slowly varying echo amplitude.[32] The low-frequency amplitude noise contributes the largest portion of the noise modulation density and is concentrated mainly below about 10 Hz at X band. The amplitude-noise spectrum is similar for both large and small targets. This is because the rate of relative range change is a function of both angular yaw and distance from the center of gravity of the aircraft. Thus, a larger aircraft with slow yaw rates but greater wingspan generates a low-frequency noise spectrum similar to that of a small aircraft with high yaw rates but smaller wingspan. However, the larger aircraft typically has the broader noise spectrum because of the difference in distribution of dominant reflectors.

The radar frequency affects the low-frequency amplitude-noise spectrum shape where the spectrum width is closely proportional to the radar frequency (if the target span is assumed to be at least several wavelengths). The reason for this dependence is that the relative phase of the individual echo signals is a function of the number of wavelengths of change in relative range caused by the target's random motion. Thus, with shorter wavelengths, a given relative range change will subtend more wavelengths, causing higher phase rate, resulting in higher-frequency noise components. The rate of amplitude fluctuations of the envelope of the echo pulses is approximately proportional to the radar frequency.

A mathematical model of low-frequency amplitude noise of a typical aircraft is given by

$$A^2(f) = \frac{0.12B}{B^2 + f^2} \tag{9.4}$$

where $A^2(f)$ = (fractional modulation)^2/Hz
B = half-power bandwidth, Hz
f = frequency, Hz

The value of B falls typically between 1.0 Hz and 2.5 Hz at X band, with the larger aircraft at the higher values because of the larger reflectors, such as engines, spread out along the wings. These reflectors with the greater separation contribute to the higher frequencies because their relative range change is large for a given angular movement of the target. $A^2(f)$ is the modulation power density such that the spectrum may be integrated over any frequency range to find the total noise power within a frequency band of interest. Taking the square root of the value of the integral gives the rms modulation.

High-Frequency Amplitude Noise. High-frequency amplitude noise consists of both random noise and periodic modulation. The random noise is largely a result of the vibration and moving parts of the aircraft producing a relatively flat noise spectrum spread out to a few hundred Hz, depending on the type of aircraft. The rms noise density is typically a few percent of modulation per $\sqrt{\text{Hz}}$.

The periodic modulation appearing as spikes in the Figure 9.19 spectrum are caused by rapidly rotating parts of an aircraft, such as the propellers. As the echo from a propeller blade changes with aspect when it rotates, a periodic modulation

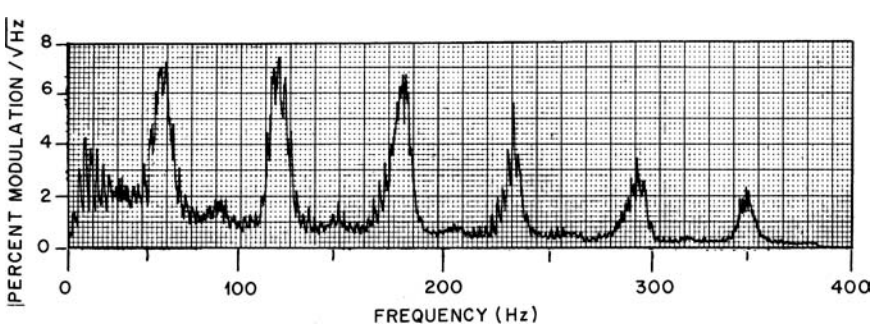

FIGURE 9.19 Typical amplitude spectral voltage distribution showing the propeller modulation measured on a propeller-driven aircraft in flight (*Figure 4 from Dunn, Howard, and King*[33] *© IRE 1959*)

is produced. The background noise from the airframe is also observed. The spikes in the spectrum result from a fundamental modulation frequency related to the propeller rev/min and number of blades. Since it is not usually sinusoidal, there are harmonic frequencies spread throughout the spectrum, as shown in Figure 9.19 for the SNB, a small aircraft with two propeller engines. The location of these spikes is not dependent on RF frequency, as in the case of low-frequency amplitude noise, because the target controls the periodicity of the modulation, which is dependent only on the aircraft propeller rotation rate and number of blades. Jet aircraft may also cause echo amplitude modulation of radar signals reflected from rotating fan blades from within the jet engines. The jet engine caused modulation is called Jet Engine Modulation (JEM) spectral modulation lines. The high-frequency-noise modulation affects scan-type tracking radars, as described later, and gives some information as to the type of aircraft.

Effects of Amplitude Scintillation on Radar Performance. Amplitude noise, to some extent, affects all types of radars in probability of detection and tracking radar accuracy.[32–36] One effect on all types of tracking radars is the interrelation between the low-frequency spectrum of amplitude noise, the AGC characteristics (which determine to what extent the slow fluctuations are smoothed), and the angle noise. The effects on angle noise are described later in this section, where it is described why a fast-acting AGC is generally the preferred choice for maximizing overall tracking accuracy.

High-frequency amplitude noise causes errors only in conical-scan or sequential lobing tracking radars because the effects are eliminated by the monopulse techniques. Conical scan or sequential lobing, to sense target direction, depend upon measuring the amplitude of the signal for at least two different antenna beam positions for each tracking axis. In azimuth tracking, for example, the antenna beam is displaced to the left of the target and then to the right. If the target were on the antenna axis, the signal would drop the same amount when the beam (assumed to be symmetrical) is moved an equal amount in either direction. The amplitudes for each beam position are subtracted in an angle error detector; hence, the output is zero if the target is on the antenna axis and becomes finite, increasing positively or negatively as the target moves off axis to the right or left.

High-frequency noise can cause the amplitude to change during the time taken to move the antenna beam from one position to the next. Even if the target is on axis, high-frequency noise can cause the amplitude at the two beam positions to differ, thus causing an erroneous indication that the target is off axis. This effect is averaged out except for the noise spectral energy near the scan rate. For example, a periodic modulation spike near the scan rate will cause the tracking radar to drive its antenna in a circular motion around the target at a rate equal to the difference in frequency between the scan rate and the frequency of the spectral line. The direction, clockwise or counterclockwise, depends upon whether the spectral line is above or below the scan rate and whether the scan is clockwise or counterclockwise. The servosystem filters out all frequencies outside the frequency range between the scan rate plus the servo bandwidth and the scan rate minus the servo bandwidth, and an angle sensitivity constant that converts rms modulation to rms angle error.

An equation using this relation to calculate rms noise in scanning and lobing-type tracking radars caused by high-frequency amplitude noise[22] is

$$\sigma_s = \frac{\theta_B}{k_s}\sqrt{A^2(f_s)\beta} \tag{9.5}$$

where σ_s = rms angle error in same angular units as θ_B
$A(f_s)$ = rms-fractional-modulation noise density in vicinity of scan rate
k_s = conical-scan error slope ($k_s = 1.6$ for system optimum[22])
θ_B = one-way antenna beamwidth
β = servo bandwidth, Hz

A sample calculation for an f_s of 120 Hz, where $A(f_s)$ from measured data taken on a large jet aircraft is approximately $0.018/\sqrt{\text{Hz}}$, θ_B is 25 mils, and β is 2 Hz, gives a σ_s of 0.42 mil rms.

In the case of a periodic modulation, where a spectral line falls within the band $f_s \pm \beta$, the rms noise is $\sigma_s = 0.67\theta_B A(f_s)$, where $A(f_s)$ is the rms fractional modulation caused by the spectral line. The resultant rms tracking error σ_s will be periodic at the frequency $f_s - f_t$ where f_t is the frequency of the spectral line.

The effects of amplitude noise on target detection and acquisition are of concern in all types of radars,[2] particularly at long ranges where the signal is weak. The amplitude fluctuations can cause the signal to drop below the noise level for short periods of time, thus affecting the choice of thresholds, acquisition scan rate, and detection logic.[34–36]

Angle Noise (Glint). Angle noise causes a change with time in the apparent location of the target with respect to a reference point on the target. This reference point is usually chosen as the *center of "gravity"* of the reflectivity distribution along the target coordinate of interest. The center of gravity is the long-time-averaged tracking angle on a target. The term *glint* is sometimes used for angle noise, but it gives the false impression that the wander in the apparent position of a target always falls within the target span. It was originally expected that angle fluctuations caused in a monopulse radar by a target would be simple variations in the center of gravity of the reflecting areas; however, much larger angle errors were observed. The apparent angular location of a target can fall at a point completely outside the extremities of the target. This can be demonstrated both experimentally and theoretically.[37,38] A pair of scatterers can be appropriately spaced to cause a tracking radar with closed-loop tracking to align its antenna axis at a point many times the scatterer spacing away from the scatterers. If the scatterers are stationary, the radar antenna will stay pointing in the erroneous direction. Figure 9.20 shows experimental data demonstrating this phenomenon with a two-reflector target.

The angle noise phenomenon affects all types of tracking radars but is mainly of concern for tracking radars where precision target location is needed. To aid in visualizing why angle noise affects any radar-type angular-direction-sensing device, the echo signal propagating in space was analyzed, showing that the angle noise is present in this propagating energy as a distortion of the phase front. Theoretical plots of a distorted phase front from dual sources compare very closely with photographs of the phase front of the radiating surface ripples in the ripple-tank experiment with dual vibrating probes.[37] All radar angle-sensing devices sense, by one means or another, the phase front of the signal and indicate the target to be in a direction normal to the phase front. Thus, the phase-front distortions affect all types of angle-sensing radars.

Many measurements of angle noise have been made on a variety of aircraft, and the results of theoretical studies have been verified. The theory and measurements show that angle noise expressed in linear units of displacement, such as meters, of the apparent position of the target from the center of gravity of the target is independent of range (except for very short ranges). Therefore, rms angle noise σ_{ang} is expressed in

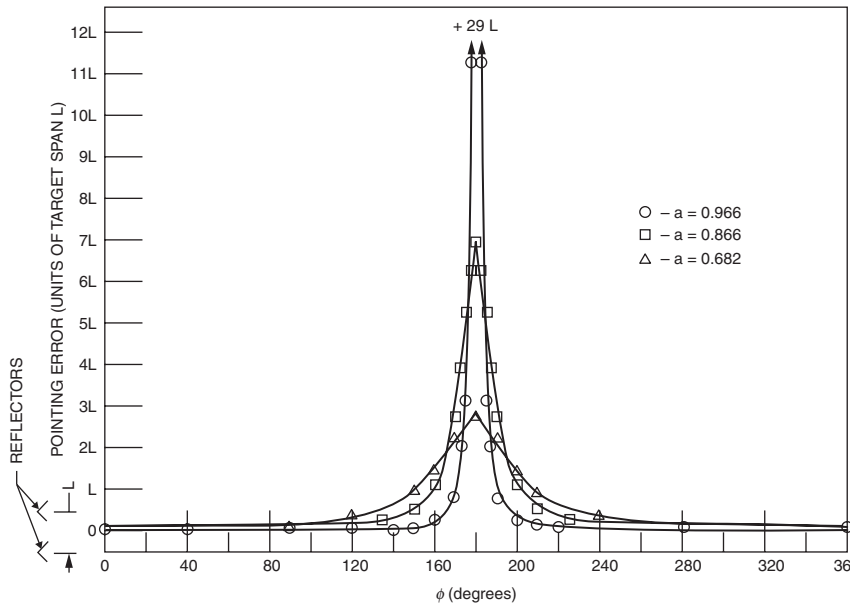

FIGURE 9.20 Apparent location of a dual-source target as a function of relative phase ϕ for different values of relative amplitude a measured with a tracking radar (*Figure 5 from Howard*[37])

units of meters of error measured at the target location. The results show that the rms value of angle noise σ_{ang} is equal to $R_o/\sqrt{2}$, where R_o is the radius-of-gyration* (taken along the angular coordinate of interest) of the distribution of the reflecting areas of the target.[33] For example, if a target's reflecting areas have a $\cos^2(\pi\alpha/L)$-shaped distribution, where α is a variable and the target span is from $+L/2$ to $-L/2$, calculation of the radius of gyration divided by $\sqrt{2}$ gives a value of σ_{ang} of $0.19L$. Typical values of σ_{ang} on actual aircraft fall between $0.15L$ and $2.0L$, depending upon the distribution of the major reflecting areas such as engines, wing tanks, and so on. A small aircraft, nose-on view, with a single engine and no significant reflectors attached to the wings will have a σ_{ang} of approximately $0.1L$, whereas larger aircraft with an outboard engine and possibly wing tanks will have a σ_{ang} approaching the value of $0.2L$. The aircraft side view also tends toward the value of $0.2L$ because of a more continuous distribution of reflecting areas. Estimation of angle scintillation rms error in units of target span can be made by relating the approximate target distribution in Figure 9.21 with actual aircraft configurations.

The value of σ_{ang} for a complex target is essentially a fixed value regardless of RF frequency, if a target span of at least several wavelengths is assumed and is independent of the rate of random motion of the target. However, as described later, the spectral distribution of angle-noise power is directly affected by radar frequency, atmospheric turbulence, and other parameters.

* Radius-of-gyration is calculated assuming the "weight" of the scatterers is their effective radar scattering cross section.

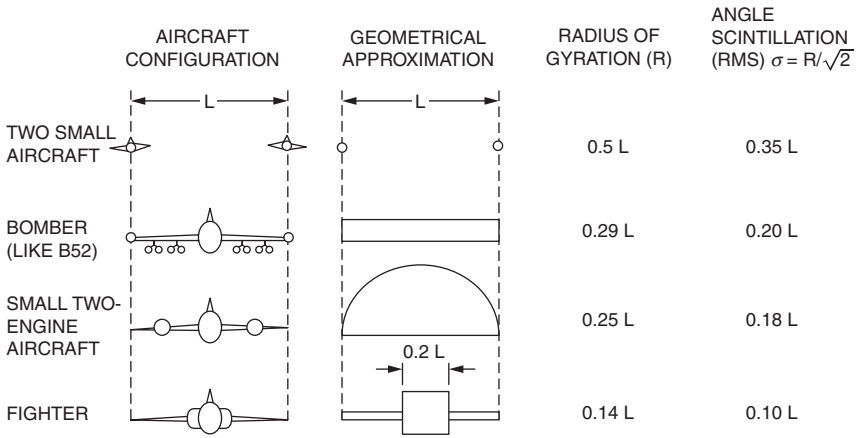

FIGURE 9.21 RMS angle scintillation based on the theoretical relation to the radius-of-gyration of the distribution of reflecting areas of the target

Target angle noise is typically gaussian-distributed. An example of the measured distribution of the apparent target angle of a small two-engine aircraft is shown in Figure 9.22. A relatively long time sample is needed, since short time samples of data can depart from the gaussian shape. Unusual targets may also depart from gaussian distributed angle noise. Delano[38] gives data from two aircraft in formation that are gaussian-distributed when completely unresolved, but change shape at close range where the antenna begins to resolve the two aircraft (as described in Section 9.11).

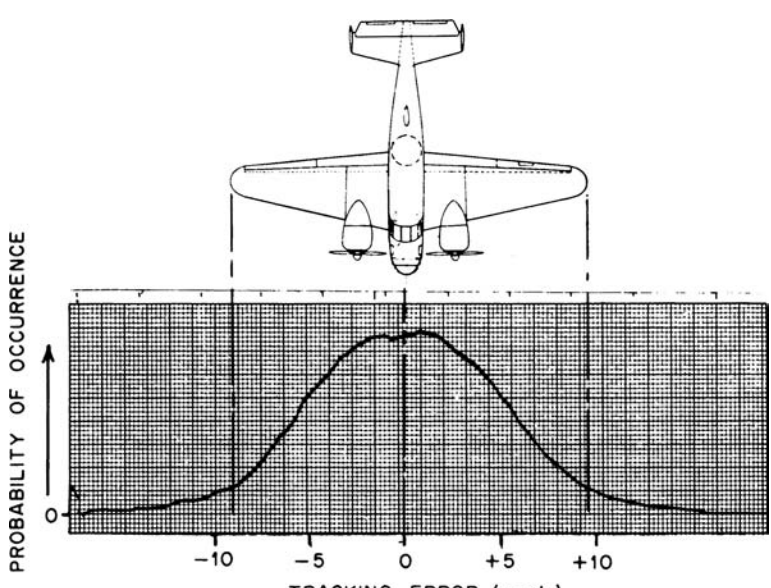

FIGURE 9.22 Amplitude probability distribution of angle scintillation measured on a small two-engine aircraft

Although the rms value of angle noise is essentially a constant for a given target and aspect, the spectral distribution of this energy is dependent on radar frequency and the random target motion. A typical spectrum shape is

$$N(f) = \sigma_{\text{ang}}^2 \frac{2B}{\pi(B^2 + f^2)} \tag{9.6}$$

where $N(f)$ = spectral noise power density, power/Hz
B = noise bandwidth, Hz
f = frequency, Hz

The values of B are proportional to radar frequency and dependent upon air turbulence effects on target motion and target aspect. An example of a measured angle scintillation spectrum is shown in Figure 9.23. Typical values of B at X band, in relatively turbulent air, range from about 1.0 Hz for small aircraft to about 2.5 Hz for larger aircraft. B changes in proportion to radar frequency provided that the target span is at least a few wavelengths. Again, long time samples are necessary to obtain a relatively smooth spectrum from measured data. For the above values of B, about 7 minutes of data was necessary to reach essentially the long-time-averaged characteristic. This is a reference point about which there will be considerable variation for a typical time period of interest. For example, with only 1 minute of data the noise power σ_{ang} would vary over 0.5 to 1.5 times the long-time-averaged σ_{ang}. At lower radar frequencies and in less turbulent atmosphere, B may be smaller, and proportionately longer time samples are necessary; thus, for short time samples of radar performance, significant statistical variations must be expected.

To convert σ_{ang} expressed in linear units measured at the target to angular units for a radar at range r, the following relation may be used:

$$\sigma_{\text{ang}}\,(\text{angular mils}) = \sigma_{\text{ang}}\,(\text{m})/r(\text{km})$$

Because the angular errors caused by angle noise are inversely proportional to range, angle noise is of concern mainly at medium and close ranges. The resultant tracking noise can be reduced by lowering the servo bandwidth to reduce the radar's ability to follow the higher-frequency components of the noise. The amount of noise reduction may be estimated by comparing the area under a spectral-power-density plot of angle noise below the frequency corresponding to the radar servo bandwidth with the total area under the power-density plot. (The spectral-power-density plot may be obtained by squaring the ordinate values of a spectral-distribution plot such as shown in Figure 9.23).

The choice of AGC characteristics also affects the amount of angle noise followed by a tracking antenna. The AGC voltage is generated from the sum signal and follows the echo-signal-amplitude fluctuation. There is a degree of correlation between the angle-noise magnitude and echo-signal magnitude such that angle-noise peaks are generally accompanied by a dip or fade in amplitude. A slow AGC system that does not maintain constant signal level during rapid changes allows the signal level to drop during a rapid fade, reducing sensitivity (volts per degree angle error) during the large angle-noise peaks. This results in a smaller rms tracking noise with a slow AGC system.[39,40]

However, this reasoning neglects an additional noise term, caused by the lack of full AGC action, which is proportional to tracking lag. A tracking lag causes a dc error

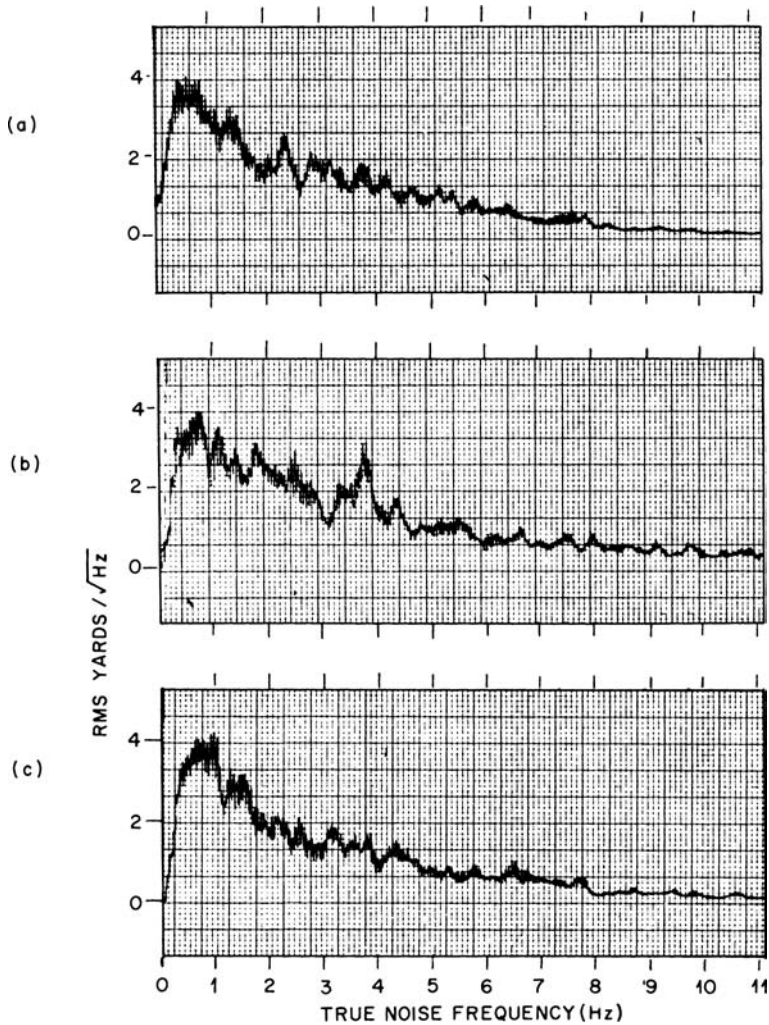

FIGURE 9.23 Spectral-energy distribution of angle scintillation measured on the nose aspect of a small two-engine aircraft

voltage in the angle-error-detector output equal to angle error times the angle sensitivity. A slow AGC allows the amplitude noise to modulate the true tracking-error voltage, causing additional noise in angle tracking. Thus, there will be an additional rms angle error proportional to tracking lag and dependent on the AGC time constant,[40] as illustrated in Figure 9.24.

In general, a fast AGC is recommended because it reduces the additional noise term allowed by slow AGC and the possibility of larger rms tracking errors, which can be considerably greater than the angle noise with a fast AGC. As previously discussed, angle noise is significant, mainly at medium and close range where target angle rates are greatest. As seen in Figure 9.24 a tracking lag of only one-half the

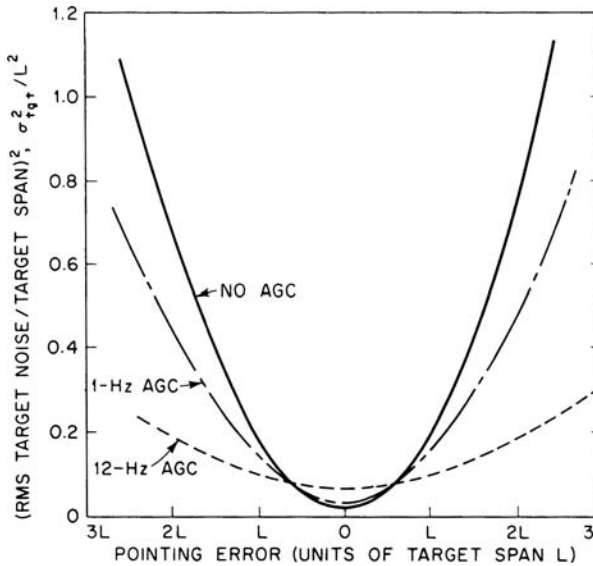

FIGURE 9.24 Angle-scintillation noise power as a function of tracking error for three different AGC bandwidths (*from Dunn, Howard, and King*[33] *© IRE 1959*)

target span will result in greater tracking noise in a slow AGC system, with the danger of much higher noise with greater lag. Therefore, for overall performance, a fast AGC is recommended.

Range Noise (Range Glint). Range noise, or random tracking errors in the range coordinate caused by complex targets, is a significant basic limitation in range tracking. Acquisition of a desired spectral line by a doppler frequency tracking system is also limited by range noise. Coarse velocity information is obtained by differentiation of range to determine the desired spectral line. Range noise is a major limitation to the accuracy of velocity obtained from range rate and can prevent selection of the desired spectral line.

The range-tracking errors caused by a finite-size target and by multipath also cause significant angle-tracking errors in multilateration tracking systems that triangulate using high-precision range measurements from multiple locations to calculate target angle location. Multilateration systems, such as the Pacific Missile Range Extended Area Tracking System (EATS), depend upon very precise range measurements. Small range-tracking errors cause significant errors in calculated target angle based on the range measurements. These errors must be fully understood to assess the performance of multilateration systems.

Target-caused range-tracking errors, similar to target-caused angle errors, are greater than the wander of the target center of gravity and can fall outside the target span.[41] Figure 9.25 shows typical samples of spectral-energy distributions and probability density functions for different target configurations. The range noise measurements were made on small and large aircraft and multiple aircraft using the split video range error detector.[42] The characteristics follow very closely to the relations of target angle noise to the target configuration radius-of-gyration along the angle coordinate.

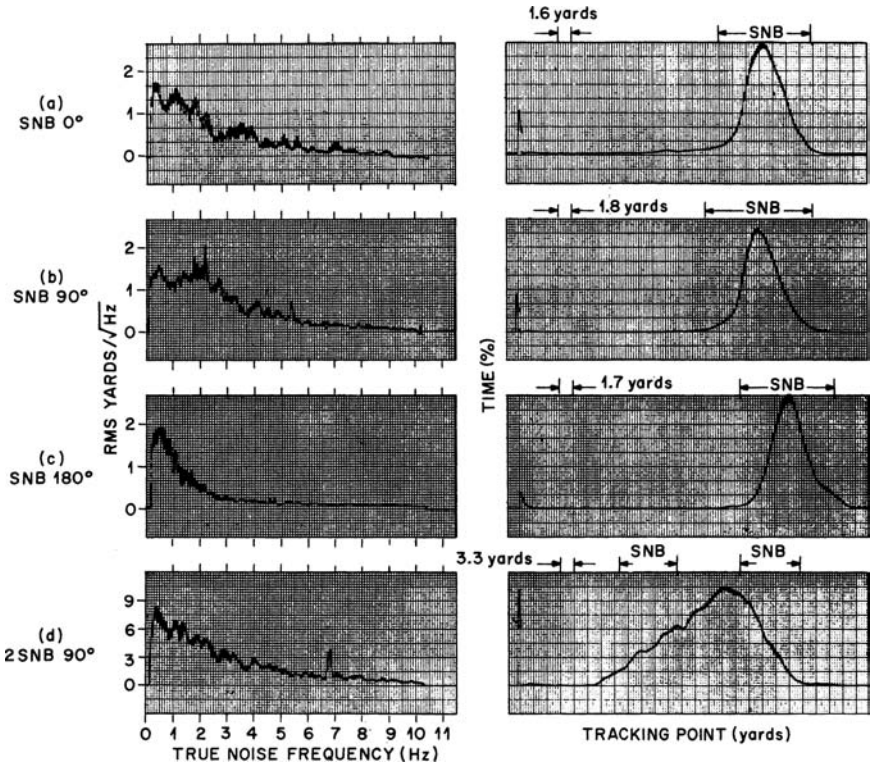

FIGURE 9.25 Typical spectral-energy distributions for the three views of the SNB aircraft: (*a*) nose view, (*b*) side view, (*c*) tail view, and (*d*) side view of two small two-engine aircraft flying in formation

For range tracking, it is necessary to relate range noise to the target reflectivity distribution along the range coordinate. In general, the long-time-average value of the rms range error may be closely estimated by taking 0.8 times the radius-of-gyration of the distribution of the reflecting areas in the range dimension based on many measurements of small, large, and multiple aircraft. Typically, in terms of target span along the range coordinate, the rms value will fall between 0.1 and 0.3 times the target span—being close to the multiplier, 0.3, for the tail view and nose view, and 0.1, for the side view. The spectral shape may be closely estimated by using the same function of frequency as described for angle noise and the same value of bandwidth. The error as a function of relative phase and amplitude of the target reflectors is similar to the angle noise phenomenon.

A beacon on a cooperative target can provide a point source (single-pulse response) to eliminate range error caused by the target. However, very stable circuitry is required to avoid pulse jitter and drift.

Doppler Scintillation and Spectral Lines. Doppler scintillation and spectral lines caused by a complex target may be divided into two phenomena[43]: (1) spectral lines caused by parts of the aircraft such as propellers and jet turbine blades, and (2) a continuous doppler spectrum spread by the motion of an aircraft in flight symmetrically

above and below the average doppler of the target. A target typically has a significant random yaw, pitch, and roll motion even on a "fixed" heading. Time plots of typical aircraft heading for an aircraft flying a "straight course" are observed to have typical random yaw motion that causes small changes in the doppler from each of the scattering surfaces of the aircraft's rigid structure. Relative to the average doppler of the aircraft, the scattering surfaces located away from the aircraft center will have a small increasing and decreasing relative doppler frequency as the aircraft yaws right and left. This causes a spectral spread of the doppler of the echo from the rigid body of the aircraft and is accompanied by spectral lines caused by moving parts on the aircraft.

Components of the target echo from rotating or moving parts of the target cause doppler lines at frequencies displaced from the airframe doppler spectrum. The periodic amplitude modulation causes pairs of doppler lines symmetrical about the doppler of the airframe velocity. Moving parts can also cause pure frequency modulation that will result in a single set of doppler lines on one side of the airframe doppler spectrum.[43]

A major significance of the doppler modulation is its effect on doppler-measuring radars. A doppler tracking system that automatically tracks the frequency of a spectral line of the echo is subjected to two problems: (1) there is the possibility of locking on a false line caused by moving parts of the target; and (2) when properly locked onto the airframe doppler spectrum, the doppler reading will be noisy as defined by the random fluctuation in instantaneous frequency as observed by the spread of the doppler spectrum. Coherent beacons (which receive, amplify, and transmit received radar pulses) can provide a doppler-shifted response free of target-caused spectral spread and periodic modulations. A delay time is provided to separate the beacon response from the target echo.

Target doppler scintillation also offers useful information about the target configuration. Normal target motion will result in different doppler shifts for each major scatterer of a rigid-body target, and the shifts will be a function of the displacement of the scatterer from a reference point such as the center of rotation of the target's random motions. Therefore, a high-resolution doppler system can resolve major reflectors and locate them in cross range as a function of the doppler difference from the reference reflector. This technique, called *inverse synthetic aperture radar (ISAR),* uses the target motion for the needed aspect change, instead of radar motion as used in conventional synthetic aperture radar, to obtain detailed cross-range target image information.[44,45]

9.9 OTHER EXTERNAL CAUSES OF ERROR

Multipath. Multipath angle errors result from reflections of the target echo from objects or surfaces causing echo pulses to arrive by other than the direct path to the radar beam in addition to the direct path. These errors are sometimes called *low-angle tracking errors* when applied to tracking of targets at small elevation angles over the Earth or ocean surface.[46–50] Multipath errors are typically a special dual-source case of angle noise resulting from the geometry as described in Figure 9.26, where the target and its image reflected from a

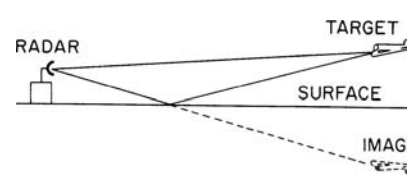

FIGURE 9.26 Geometry of the radar multipath tracking condition, where the reflection from a surface appears to the radar as an image below the surface

surface to the radar beam are the two sources. Over a smooth ocean surface, they are separated only in the elevation coordinate so that most of the error appears in the elevation-tracking channel. Severe elevation errors may cause some cross coupling of the error to the azimuth channel. Rough surfaces cause diffuse scattering, which can contribute errors to both azimuth and elevation tracking.[46] Different path geometries such as non-flat land or a building may also cause a significant error to appear in the azimuth-tracking channel.

The major difficulty with low-angle tracking is that the target and its image are essentially coherent and their relative phase changes slowly and the angular error it causes is readily followed by an angle-tracking system. Furthermore, the paths are almost equal, and in most cases, they cannot be resolved by high-range-resolution techniques. Long time averages of the data do not, in practice, give target elevation; thus, the multipath angle error has no simple solution and is generally minimized by using narrow-beam antennas.

When the target is at low altitude, the multipath errors are severe, as observed in the measured data shown in Figure 9.27. This data is the multipath error of a 2.7° beamwidth S band (3-GHz) tracking radar that is tracking an aircraft target with a beacon at 3300-ft altitude. An AN/FPS-16 tracking radar with a 1.1° beamwidth at C band (5.7 GHz) was used to simultaneously track with its narrow beam, which remained above the sea surface without significant multipath error, to provide a true target altitude reference for the data in Figure 9.27. There is a measurement bias error (observed in Figure 9.27) of about 0.25°.

The tracking data from a radar tracking a target with a beacon is plotted in Figure 9.27, showing a typical multipath error illustrating the phenomenon from the region where the image enters the sidelobes to the region where it enters the main beam. There are three methods used for predicting multipath errors, depending upon where the reflected target image enters the antenna pattern. At the far range,

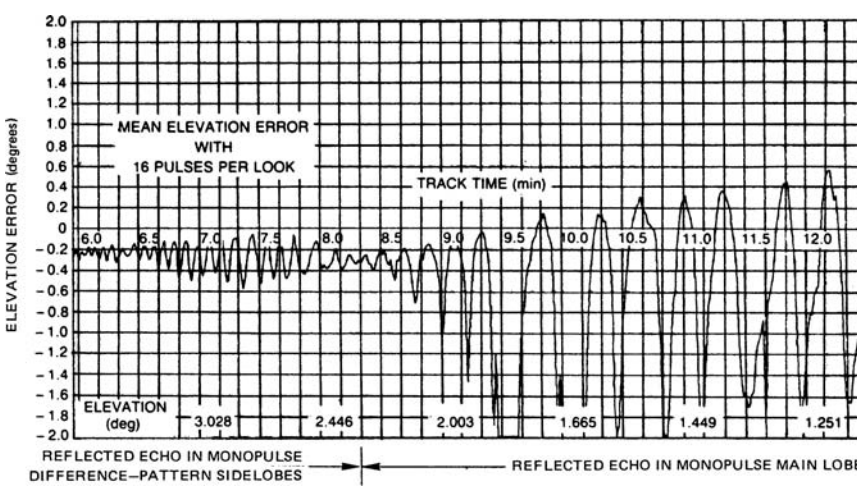

FIGURE 9.27 Measured elevation-tracking error of an S-band radar using an AN/FPS-16 radar for a target elevation reference

the image enters the antenna main beam, and the error is essentially that of a two-reflector target glint error following approximately the equation[37]

$$e = 2h\frac{\rho^2 + \rho\ \cos\phi}{1 + \rho^2 + 2\rho\ \cos\phi} \tag{9.7}$$

where e = error, same units as h, measured at the target range relative to the target
ρ = magnitude of surface reflection coefficient
h = height of target
ϕ = relative phase determined by geometry of direct and surface-reflected signal paths, as shown in Figure 9.26.

Although the fluctuations in ρ and ϕ alter the actual tracking from the theoretical, the equation gives a good indication of the errors to be expected when tracking a point source such as a beacon. However, skin tracking of an aircraft at low elevation may result in a departure from the classic periodic error versus elevation, as illustrated in Figure 9.27, because of an interaction between target angle scintillation and multipath error that can change the characteristics of the multipath error.

When tracking a point source target at close range, the radar main beam is above the image, but the image is seen by the difference-pattern sidelobes. The multipath errors that result are cyclic, almost sinusoidal, with an rms value predicted by the equation[46]

$$\sigma_E = \frac{\rho\theta_B}{\sqrt{8G_{se}(\text{peak})}} \tag{9.8}$$

where σ_E = rms elevation angle multipath error, same units as θ_B
θ_B = one-way antenna beamwidth
ρ = reflection coefficient

and G_{se} (peak) is the power ratio of the tracking-antenna sum-pattern peak to the error-pattern peak sidelobe level at the angle of arrival of the image signal.

The cyclic rate may be approximated by the equation

$$f_m = \frac{2hE}{\lambda} \tag{9.9}$$

where f_m = frequency of cyclic multipath error, rad/s
h = height of radar antenna
λ = wavelength, same units as h
E = rate of target elevation change as seen by radar, rad/s

The intermediate range is between the short-range region where the image appears in the sidelobes, and the long-range region, where the image appears within the half-power beamwidth. The error is difficult to calculate in this region because it falls in the nonlinear error-sensing portion of the antenna patterns, and the radar response is strongly dependent upon the specific feed design and error-processing technique. However, Figure 9.28[46,47] provides a practical means for approximating multipath-error values in this region. The curves are calculated multipath errors based on an assumed gaussian-shaped sum pattern and derivative of the sum pattern

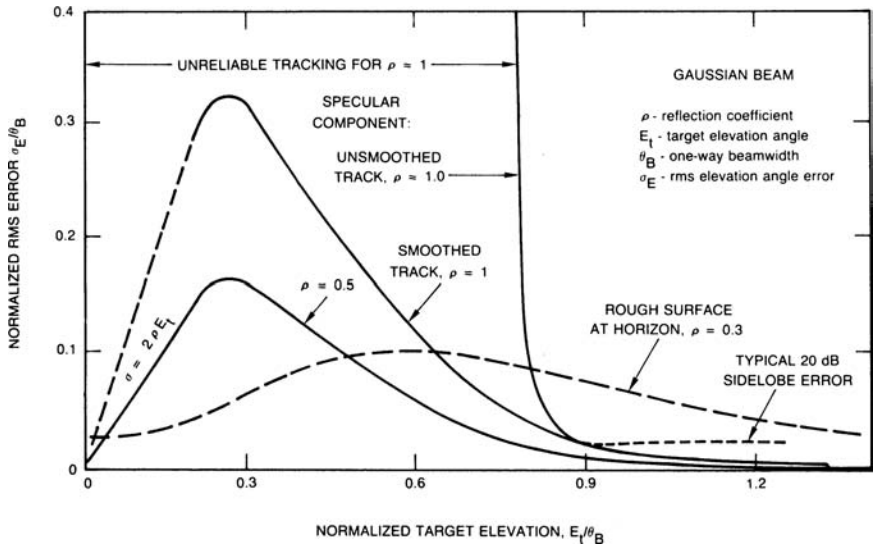

FIGURE 9.28 Calculated rms multipath error σ_E versus target elevation E_t, both normalized to radar beamwidth θ_B

as the monopulse difference pattern. Figure 9.28 shows typical sidelobe multipath errors for higher-elevation targets and the linearly decreasing error versus target elevation, predicted by the above equation, for very low-elevation targets. The graph is normalized to radar beamwidth on both axes for convenient use with a wide variety of radars. The dashed portions of the curves are regions of uncertainty because of significant variations of reflection for a given sea state.

In the intermediate region, the error increases to a peak at target elevations of about 0.3 beamwidth. The peak value is dependent on several factors including surface roughness (which, in part, determines the value of ρ), servo bandwidth, and antenna characteristics in the region. The errors are severe, and with *un-smoothed track* (wide servo bandwidth), the radar can break lock and lose track of the target.

When the surface is rough, corresponding to a reflection coefficient of about 0.3, the characteristic of the error versus elevation changes is observed in Figure 9.28. The rough surface causes significant diffuse scattering rather than a mirror reflection. This changes the shape of the error curve and results in some residual elevation-angle error when the target elevation goes to zero. It also causes some significant azimuth error.[46]

Crosstalk Caused by Cross-Polarized Energy. Target echo energy cross-polarized to the radar antenna causes crosstalk (cross coupling) in radars; i.e., the azimuth error causes output from the elevation-error detector, and the elevation error causes output from the azimuth-error detector. Generally, this effect is negligible because the cross-polarized energy is usually a small fraction of the received polarization from typical targets, and it is normally reduced by about 20 dB by the antenna design. However, in special cases, the resultant crosstalk can be very high and may cause a large tracking error and possible loss of track. For example, polarization of a linearly polarized beacon on a target could rotate with target aspect change and, in the worst case, approach a cross-polarized condition.

Theoretically, the coupling to cross-polarized energy is zero when the source is precisely on axis and increases with displacement from the axis.[51] The cross-polarization error in a tracking radar system is pure crosstalk so that a small true tracking error in one tracking coordinate causes the antenna to move in the other coordinate. The error in the second coordinate then causes the antenna to move farther from the source in the first coordinate. When there is no retarding effect, the cross-polarized energy causes the antenna to drive off target in one of the quadrants of the two-axis angle-tracking coordinate system, depending upon the direction of the initial error that moved the source off the precise on-axis position.[4,51]

A solution used with missile-range-instrumentation radar, where target aspect changes can cause a linearly polarized beacon to rotate to a cross-polarized aspect, is to provide a circular polarization tracking capability. Coupling a linearly polarized signal to a circularly polarized antenna results in a 3 dB signal loss, but it is independent of the direction of the linear polarization when rotated about a line in the direction toward the radar.

Troposphere Propagation. The troposphere is typically a nonhomogeneous medium for propagation and will cause random beam bending. Figure 9.29 illustrates the approximate relation of rms angle error to various atmospheric conditions.[22] The worst case is heavy cumulus clouds, which cause columns of air, shaded from the sun by the clouds, that are cooler than the surrounding air and consequently of a different dielectric constant. The result is typically a random beam bending as the radiated energy passes through these columns. Figure 9.29 applies only for the portion

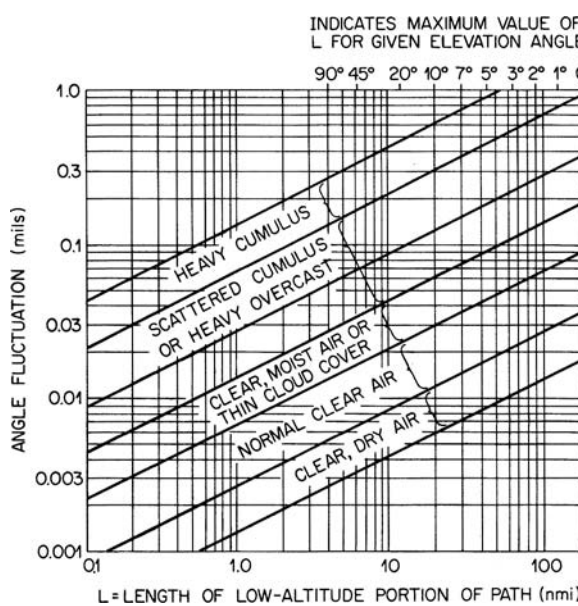

FIGURE 9.29 Angle fluctuation versus path length for different tropospheres (*from Final Report: Instrumentation Radar AN/FPS-16 (XN-2) by RCA under contract Bu Aer NOas 55-869c*)

of the beam that is within the troposphere. Once the beam goes above the troposphere (typically about 6 to 9 km), there is no further beam bending.

The troposphere also affects target range measurement, but the errors are small, in the order of 0.3 to 0.6 m maximum. However, even small errors of this magnitude will cause significant errors in multilateration systems that determine target angle by calculations using precise range measurements from separate locations.

9.10 INTERNAL SOURCES OF ERROR

Receiver Thermal Noise. The angle error caused by receiver thermal noise in a monopulse tracking system is

$$\sigma_t = \frac{\theta_B}{k_m \sqrt{B\tau(S/N)(f_r/\beta_n)}} \tag{9.10}$$

where k_m is the angle-error-detector slope. The value of k_m is determined by the steepness of the antenna difference patterns, and a variety of values can be obtained, depending on the type of feed used. The values vary from 1.2 for the original four-horn square feed to a maximum of 1.9 for the MIT 12-horn feed. However, as described in the discussion on feeds, the 12-horn feed gives a lower antenna efficiency (0.58) than an optimum multimode monopulse feed, which can approach an efficiency of 0.75, although its angle sensitivity is less, typically having a value of 1.7. Therefore, there is a tradeoff between slope and efficiency. A slope for monopulse radars is dependent upon feed design and is typically 1.57 for a good modern four-horn multimode feed design.

When there is a significant tracking lag or deliberate beam offset from the target, the error σ_{to}, due to receiver noise for a given SNR, is given by the equation

$$\sigma_{t0} = \sigma_t \sqrt{L[1 + k(\theta_L/\theta_B)^2]} \tag{9.11}$$

where θ_L = lag angle, same units as θ_B
L = antenna sum-pattern loss at angle θ_L

A similar range-tracking error σ_{rt} results from receiver noise. The equation relating the error to the SNR and system parameters is

$$\sigma_{rt} = \frac{\tau}{\sqrt{k_r(S/N) f_r/\beta_n}} \quad \text{ft (rms)} \tag{9.12}$$

where τ = pulse length in ft
k_r = range-error-detector sensitivity (maximum value of 2.5 for a receiver where $B = 1.4$)
S/N = signal-to-noise ratio
β_n = servo bandwidth

Other Internal Sources of Error. There are many other sources of internal errors that are small in well-designed tracking radars. These include changes in relative phase and amplitude between monopulse receiver channels as a function of signal strength,

TABLE 9.1 Inventory of Range-Error Components*

Component	Bias	Noise
Radar-dependent tracking errors	Zero range setting Range discriminator shift servo unbalance Receiver delay	Receiver thermal noise Multipath Servo electrical noise Servo mechanical noise Variation in receiver delay
Radar-dependent translation errors	Range oscillator frequency Data takeoff zero setting	Range resolver error Internal jitter Data gear nonlinearity and backlash Data takeoff nonlinearity and granularity Range oscillator instability
Target-dependent tracking errors	Dynamic lag Beacon delay	Dynamic lag Glint Scintillation Beacon jitter
Propagation error	Average tropospheric refraction Average ionospheric refraction	Irregularities in tropospheric refraction Irregularities in ionospheric refraction

*From D. K. Barton in "Modern Radar," R. S. Berkowitz (ed.), New York: John Wiley & Sons, 1965, chap. 7, p. 622.

RF frequency, detuning, and temperature. Also, pedestal bending from solar heating, nonorthogonality of pedestal axes, gearing backlash, bearing wobble, granularity of data readout, and many other factors contribute to errors. Table 9.1 lists the magnitude of these errors for the precision instrumentation radar AN/FPS-16.[22]

Calibration is important to minimize errors.[22] When maximum performance is required, timely accurate calibration must be performed. The procedure may require up to four hours to fully stabilize the radar system. For instrumentation radar, where the time of a tracking event is known, final calibration is performed just preceding the event to minimize drift errors.

9.11 SUMMARY OF SOURCES OF ERROR

Angle Measurement Errors. An inventory of angle measurement errors is given in Table 9.2. This includes several sources of error that should be considered in addition to the radar-related sources.

Figure 9.30 is an example of the measured tracking performance of an AN/FPS-16 radar tracking a 6-in metal sphere that provides a point source target to eliminate target-caused errors. The data illustrates which error sources dominate at different regions of the radar range and their characteristics versus range.

The target-caused errors discussed in Section 9.8 include the usual tracking events where the target extent is within the 3-dB beamwidth of the radar. However, a large target such as an aircraft formation may extend beyond the linear angle-error region of the antenna patterns and eventually reach the point of resolution of one of the aircraft. The resultant angle-tracking error for large targets is illustrated by the example in Figure 9.31. In Figure 9.31*a,* the typical gaussian-like glint error distribution is observed. With the wider separation of the aircraft, the tracking-error

TABLE 9.2 Inventory of Angle-Error Components*

Component	Bias	Noise
Radar-dependent tracking errors (deviation of antenna from target)	Boresight axis collimation Axis shift with RF and IF tuning Receiver phase shift Target amplitude Temperature Wind force Antenna unbalance Servo unbalance	Receiver thermal noise Multipath (elevation only) Wind gusts Servo electrical noise Servo mechanical noise
Radar-dependent translation errors (errors in converting antenna position to angular coordinates)	Leveling of pedestal North alignment Static flexure of pedestal and antenna Orthogonality of axes solar heating	Dynamic deflection of pedestal and antenna Bearing wobble Data gear nonlinearity and backlash Data takeoff nonlinearity and granularity
Target-dependent tracking errors	Dynamic lag	Glint Dynamic lag variation Scintillation Beacon modulation
Propagation errors	Average refraction of troposphere Average refraction of ionosphere	Irregularities in tropospheric refraction Irregularities in ionospheric refraction
Apparent or instrumentation errors (for optical reference)	Telescope or reference instrument stability Film emulsion and base stability Optical parallax	Telescope, camera, or reference instrument vibration Film-transport jitter Reading error Granularity error Variation in optical parallax

*From D. K. Barton in "Modern Radar," R. S. Berkowitz (ed.), New York: John Wiley & Sons, 1965, chap. 7, p. 618.

distribution changes shape, becoming somewhat rectangular with a separation of aircraft as in Figure 9.31*b*. At the widest separation, where the aircraft are almost resolved, as in Figure 9.31*c*, the radar will track one aircraft until it fades and the other aircraft blossoms in amplitude. Then the radar-tracking point will move to the other aircraft. The dwell on each target with random switching between the two aircraft causes the double-humped distribution of error.

Range Measurement Errors. The major sources of target range-error measurement errors are given in Table 9.3. Typical bias and noise of target range measurement errors in a precision-ranging radar are equal to a total rms value of 1.6 m rms. Further details of range-error sources and their magnitude are give in Section 10.3 of Barton.[22]

Limitations of Performance. Mitchell et al.[52] describe basic performance limitations of the AN/FPQ-6 high precision tracking radar measured under ideal

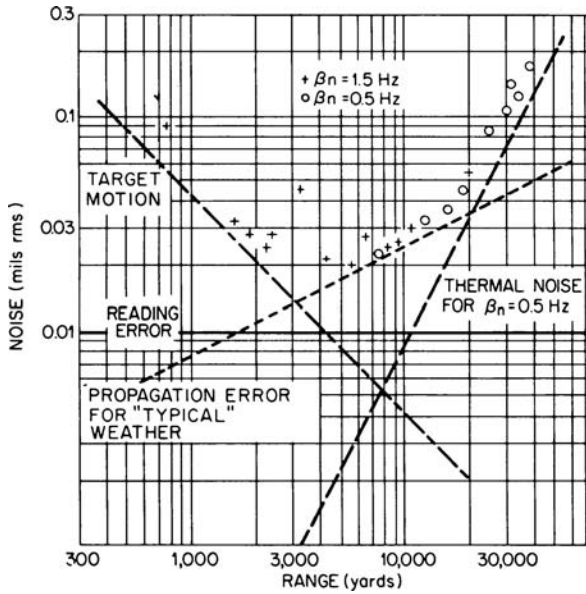

FIGURE 9.30 Azimuth-tracking noise versus range using a 6-in metal sphere target supported inside a balloon to minimize target motion (estimated at 1.5 in rms). β_n = servo bandwidth

conditions with a carefully designed boresighting facility. This task provided measured data verifying the anticipated performance of the highest precision tracking radar at that time.

TABLE 9.3 Inventory of Range-Error Components*

Component	Bias	Noise
Radar-dependent tracking errors	Zero range setting Range discriminator shift servo unbalance Receiver delay	Receiver thermal noise Multipath Servo electrical noise Servo mechanical noise Variation in receiver delay
Radar-dependent translation errors	Range oscillator frequency Data takeoff zero setting	Range resolver error Internal jitter Data gear nonlinearity and backlash Data takeoff nonlinearity and granularity Range oscillator instability
Target-dependent tracking errors	Dynamic lag Beacon delay	Dynamic lag Glint Scintillation Beacon jitter
Propagation error	Average tropospheric refraction Average ionospheric refraction	Irregularities in tropospheric refraction Irregularities in ionospheric refraction

*From D. K. Barton in "Modern Radar," R. S. Berkowitz (ed.) New York: John Wiley & Sons, 1965, chap. 7, p. 622.

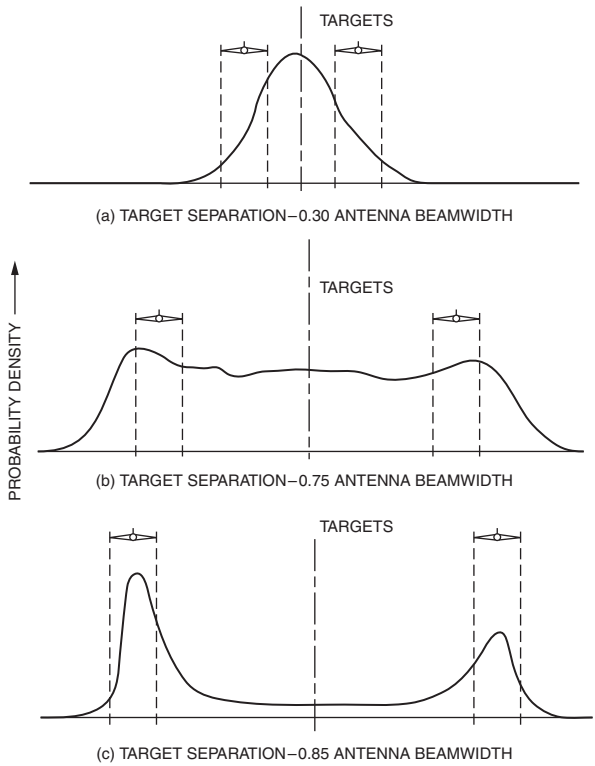

FIGURE 9.31 Probability distribution of radar pointing when tracking two targets (where the left target is approximately 1.5 dB larger than the right target). Three different angular separations of the targets are (*a*) 0.30 antenna beamwidth, (*b*) 0.75 antenna beamwidth, and (*c*) 0.85 antenna beamwidth.

9.12 ERROR REDUCTION TECHNIQUES

Multipath-Error Reduction. Very-low-altitude targets cause severe elevation-angle tracking errors, as described in Section 9.9, which may result in useless elevation tracking data and possible loss of tracking of the target. A variety of techniques have been developed to reduce these errors or their effects on radar tracking.[53–58] One simple approach to avoid loss of tracking in elevation is to open the elevation-tracking servo loop and place the antenna beam at about a half beamwidth above the horizon.[1] Azimuth closed-loop tracking may continue. Although the elevation-angle-error-detector output has large indicated angle errors, it is monitored to observe whether or not the target is maneuvering upward through the beam. A target rising through the beam will cause a positive angle-tracking error indication and the closed-loop elevation tracking resumes.

A very effective and direct approach to multipath-error reduction is to use a very narrow beam, usually accomplished by operating at short wavelengths such as an 8-mm (35 GHz or K_a band) region with the usual microwave-tracking aperture size.[13,25,26,

This approach can reduce errors by two effects. First, as observed in Figure 9.28, the magnitude of the elevation multipath error reduces in direct proportion to the beamwidth. The second advantage of shorter wavelengths is that even a relatively smooth sea, such as sea state 1, has wave heights of many wavelengths and appears rough, resulting in a smaller reflection coefficient. This is observed in Figure 9.28 to give small multipath errors. The 8-mm-wavelength monopulse capability may be effectively combined with a lower microwave band as described in Section 9.6 to take advantage of the complementary features of both bands.

Target Angle and Range Scintillation (Glint) Reduction. Target-caused errors in angle and range tracking may be reduced by filtering, such as reducing tracking servo bandwidth. However, sufficient servo bandwidth must be retained to follow target trajectories. Unfortunately, target angle and range scintillation power density is normally concentrated below about 1 to 2 Hz when operating at microwave bands and falls within normally required bandwidths.

Target scintillation total noise power is relatively independent of frequency, but the spectral energy tends to spread upward in frequency as wavelength is reduced, resulting in lower noise power density in the servo passband. Therefore, operating at a shorter wavelength will result in lower target noise effects on closed-loop tracking.

Diversity techniques, which can provide statistically independent samples of target scintillation, offer a means for reducing target scintillation effects. The most practical technique is frequency diversity using pulse-to-pulse radar frequency change, which will alter the phase relations between the echoes from dominant reflecting surfaces of the target.[59–62] The frequency change must be sufficient to cause enough change in relative phases of the reflectors to result in statistically independent samples of target scintillation at each new frequency. An approximate rule is a minimum frequency change of $1/\tau$, where τ is the radar range delay time between the leading and lagging extremities of the target. The reduction in rms angle and range target scintillation may be approximated by dividing by the square root of n, where n is the number of frequency steps provided.

Reduction of Internally Caused Errors. Angle errors caused by receiver thermal noise, as well as target scintillation, are minimized by maintaining the target as closely as possible to the tracking axes. The technique called *on-axis tracking,* described in Section 9.6, is a means of placing a computer in the tracking loop to minimize lag and provide optimum angle-error filtering.

Accurate system calibration also greatly reduces internal sources of error. Frequent calibration corrects for drift in component gain and phase and pedestal flexure. Other internal sources of error with known characteristics can be automatically corrected to minimize their contamination of the output data.

REFERENCES

1. S. M. Sherman, *Monopulse Principles and Techniques*, Norwood, MA: Artech House, 1986.
2. A. I. Leonov and K. I. Formichev, *Monopulse Radar*," Norwood, MA: Artech House, 1986.
3. J. H. Dunn and D. D. Howard, "Precision tracking with monopulse radar," *Electronics*, vol. 33, pp. 51–56, April 22, 1960.
4. P. Z. Peebles, Jr., "Signal Processor and accuracy of three-beam monopulse tracking radar," *IEEE Trans*., vol. AES-5, pp. 52–57, January 1969.

5. P. W. Hannan, "Optimum feeds for all three modes of a monopulse antenna, I: Theory; II: Practice," *IEEE Trans*., vol. AP-9, pp. 444–460, September 1961.
6. "Final report on instrumentation radar AN/FPS-16 (XN-2)," Radio Corporation of America, unpublished report NTIS 250500, pp. 4-123–4-125.
7. D. K. Barton, "Recent developments in radar instrumentation," *Astron. Aerosp. Eng*., vol. 1, pp. 54–59, July 1963.
8. J. T. Nessmith, "Range instrumentation radars," *IEEE Trans*., vol. AES-12, pp. 756–766, November 1976.
9. J. A. DiCurcio, "AN/TPQ-27 precision tracking radar," in *IEEE Int. Radar Conf. Rec*., Arlington, VA, 1980, pp. 20–25.
10. D. D. Howard, "Single Aperture monopulse radar multi-mode antenna feed and homing device," in Proc. *IEEE Int. Conv. Mil. Electron. Conf*., September 14–16, 1964, pp. 259–263.
11. P. Mikulich, R. Dolusic, C. Profera, and L. Yorkins, "High gain cassegrain monopulse antenna," in *IEEE G-AP Int. Antenna Propag. Symp. Rec*., September 1968.
12. R. C. Johnson and H. Jasik, *Antenna Engineering Handbook*, 2nd Ed., New York: McGraw-Hill Book Company, 1984, Chap. 34.
13. D. Cross, D. Howard, M. Lipka, A. Mays, and E. Ornstein, "TRAKX: A dual-frequency tracking radar," *Microwave J*., vol. 19, pp. 39–41, September 1976.
14. V. W. Hammond and K. H. Wedge, "The application of phased-array instrumentation radar in test and evaluation support," in *Electron. Nat. Security Conf. Rec*., Singapore, January 17–19, 1985.
15. J. W. Bornholdt, "Instrumentation radars: Technical evaluation and use," in *Proc. Int. Telemetry Council*, November 1987.
16. W. B. Milway, "Multiple target instrumentation radars for military test and evaluation," in *Proc. Int. Telemetry Conf*. vol. XXI, 1985.
17. R. L. Stegall, "Multiple object tracking radar: System engineering considerations," in *Proc. Int*. Telemetry Council, 1987.
18. R. S. Noblit, "Reliability without redundancy from a radar monopulse receiver," *Microwaves*, pp. 56–60, December 1967.
19. H. Sakamoto and P. Z. Peebles, Jr., "Conopulse radar," *IEEE Trans*., vol. AES-14, pp. 199–208, January 1978.
20. P. A. Bakut and I. S. Bol'shakov, *Questions of the Statistical Theory of Radar*, vol. II, Moscow: Sovetskoye Radio, 1963, Chaps. 10 and 11. (Translation available from NTIS, AD 645775, June 28, 1966.)
21. M. I. Skolnik, *Introduction to Radar Systems*, 2nd Ed., New York: McGraw-Hill Book Company, 1980.
22. D. K Barton, *Radar Systems Analysis*, Norwood, MA: Artech House, 1977.
23. A. S. Locke, *Guidance, Princton*, NJ: D. Van Nostrand Company, 1955, Chap. 7.
24. D. C. Cross, "Low jitter high performance electronic range tracker," in *IEEE Int. Radar Conf. Rec*., 1975, pp. 408–411.
25. D. L. Malone, "FLYCATCHER," *Nat. Def*., pp. 52–55, January 1984.
26. Hollandse Signaalapparaten B.V. advertisement, *Def. Electron*., vol. 19, p. 67, April 1987.
27. Editor, "Inside the Exocet: Flight of a sea skimmer," *Def. Electron*., vol. 14, pp. 46–48, August 1982.
28. Editor, "Special series: Israeli Avionics-2," *Aviat. Week Space Technol*., pp. 38–49, April 17, 1978.
29. D. C. Cross, D. D. Howard, and J. W. Titus, "Mirror-antenna radar concept," *Microwave J*., vol. 29, pp. 323–335, May 1986.
30. D. D. Howard and D. C. Cross, "Mirror antenna dual-band light weight mirror design," *IEEE Trans*., vol. AP-33, pp. 286–294, March 1985.
31. E. P. Schelonka, "Adaptive control technique for on-axis radar," in *Int. Radar Conf. Rec*., 1975 pp. 396–401.

32. I. D. Olin and F. D. Queen, "Dynamic measurement of radar cross section," *Proc. IEEE*, vol. 53, pp. 954–961, August 1965.
33. J. H. Dunn, D. D. Howard, and A. M. King, "Phenomena of scintillation noise in radar-tracking systems," *Proc. IRE*, vol. 47, pp. 855–863, May 1959.
34. M. I. Skolnik, *Introduction to Radar Systems*, New York: McGraw-Hill Book Company, 1962, Chap. 2.
35. D. K. Barton, *Modern Radar System Analysis*, Norwood, Mass: Artech House, 1988, p. 388.
36. G. Merrill, D. J. Povejsil, R. S. Raven, and P. Waterman, *Airborne Radar*, Boston: Boston Technical Publishers, 1965, pp. 203–207.
37. D. D. Howard, "Radar target angular scintillation in tracking and guidance systems based on echo signal phase front distortion," in *Proc. Nat. Electron. Conf.*, vol. 15, October 1959.
38. R. H. Delano, "A theory of target glint or angle scintillation in radar tracking," *Proc. IRE*, vol. 41, pp. 1778–1784, December 1953.
39. R. H. Delano and I. Pfeffer, "The effects of AGC on radar tracking noise," *Proc. IRE*, vol. 44, pp. 801–810, June 1956.
40. J. H. Dunn and D. D. Howard, "The effects of automatic gain control performance on the tracking accuracy of monopulse radar systems," *Proc. IRE*, vol. 47, pp. 430–435, March 1959.
41. D. C. Cross and J. E. Evans, "Target generated range errors," in *IEEE Int. Radar Conf. Rec.*, Arlington, VA, April 21–23, 1975, pp. 385–390.
42. D. J. Povejsil, R. S. Raven, and P. Waterman, *Airborne Radar*, Princeton, NJ: D. Van Nostrand Company, 1961, pp. 397–399.
43. R. Hynes and R. E. Gardner, "Doppler spectra of S band and X band signals," *IEEE Trans. Suppl.*, vol. AES-3, pp. 356–365, November 1967.
44. A. A. Ausherman, A. Kozma, J. L. Walker, H. M. Jones, and E. C. Poggio, "Development in radar imaging," *IEEE Trans.*, vol. AES-20, pp. 363–400, July 1984.
45. G. Dike, R. Wallenberg, and J. Potenza, "Inverse SAR and its application to aircraft classification," in *IEEE Int. Radar Conf. Rec.*, pp. 20–25, 1980.
46. D. K. Barton, "The low-angle tracking problem," presented at *IEE Int. Radar Conf.*, London, October 23–25, 1973.
47. D. K. Barton and H. R. Ward, *Handbook of Radar Measurement*, Englewood Cliffs, NJ: Prentice-Hall, 1969.
48. D. K. Barton, "Low-angle radar tracking," *Proc. IEEE*, vol. 62, pp. 687–704, June 1974.
49. D. K. Barton, *Radar Resolution and Multipath Effects* in vol. 4 of *Radars*, Norwood, MA: Artech House, 1978.
50. D. D. Howard, J. Nessmith, and S. M. Sherman, "Monopulse tracking error due to multipath: Causes and remedies," in *EASCON Rec.*, 1971 pp. 175–182.
51. E. M. T. Jones, "Paraboloid reflector and hyperboloid lens antenna," *IRE Trans.*, vol. AP-2, pp. 119–127, July 1954.
52. R. Mitchell et al., "Measurements of performance of MIPIR (Missile Precision Instrumentation Radar Set AN/FPQ-6)," *Final Rept., Navy Contract NOW61-0428d*, RCA, Missile and Surface Radar Division, Moorestown, NJ, December 1964.
53. P. R. Dax, "Accurate tracking of low elevation targets over the sea with a monopulse radar," in *IEE Radar Conf. Publ.* 105, *Radar—Present and Future*, London, October 23–25, 1973, pp. 160–165.
54. D. D. Howard, "Investigation and application of radar techniques for low-altitude target tracking," in *IEE Int. Radar Conf. Rec.*, London, October 25–26, 1977.
55. D. D. Howard, "Environmental effects on precision monopulse instrumentation tracking radar at 35 GHz," in *IEEE EASCON '79 Rec.*, October 1979.
56. R. J. McAulay and T. P. McGarty, "Maximum-likelihood detection of unresolved targets and multipath," *IEEE Trans.*, vol. AES-10, pp. 821–829, November 1974.

57. W. D. White, "Techniques for tracking low-altitude radar targets in the presence of multipath," *IEEE Trans*., vol. AES-10, pp. 835–852, November 1974.
58. P. Z. Peebles, Jr., "Multipath error reduction using multiple target methods," *IEEE Trans*., vol. AES-7, pp. 1123–1130, November 1971.
59. F. E. Nathanson, *Radar Design Principles*, New York: McGraw-Hill Book Company, 1969, p. 37.
60. G. Linde, "Reduction of radar tracking errors with frequency agility," *IEEE Trans*., vol. AES-4, pp. 410–416, May 1968.
61. G. Linde, "A simple approximation formula for glint improvement with frequency agility," *IEEE Trans*., AES-8, pp. 853–855, November 1972.
62. D. K. Barton, *Frequency Agility and Diversity*, in Vol. 6 of *Radars*, Norwood, MA: Artech House, 1977.